



CMS-SMP-14-001

CERN-EP/2016-196
2017/04/05

Measurement and QCD analysis of double-differential inclusive jet cross sections in pp collisions at $\sqrt{s} = 8 \text{ TeV}$ and cross section ratios to 2.76 and 7 TeV

The CMS Collaboration*

Abstract

A measurement of the double-differential inclusive jet cross section as a function of the jet transverse momentum p_T and the absolute jet rapidity $|y|$ is presented. Data from LHC proton-proton collisions at $\sqrt{s} = 8 \text{ TeV}$, corresponding to an integrated luminosity of 19.7 fb^{-1} , have been collected with the CMS detector. Jets are reconstructed using the anti- k_T clustering algorithm with a size parameter of 0.7 in a phase space region covering jet p_T from 74 GeV up to 2.5 TeV and jet absolute rapidity up to $|y| = 3.0$. The low- p_T jet range between 21 and 74 GeV is also studied up to $|y| = 4.7$, using a dedicated data sample corresponding to an integrated luminosity of 5.6 pb^{-1} . The measured jet cross section is corrected for detector effects and compared with the predictions from perturbative QCD at next-to-leading order (NLO) using various sets of parton distribution functions (PDF). Cross section ratios to the corresponding measurements performed at 2.76 and 7 TeV are presented. From the measured double-differential jet cross section, the value of the strong coupling constant evaluated at the Z mass is $\alpha_S(M_Z) = 0.1164^{+0.0060}_{-0.0043}$, where the errors include the PDF, scale, nonperturbative effects and experimental uncertainties, using the CT10 NLO PDFs. Improved constraints on PDFs based on the inclusive jet cross section measurement are presented.

Published in the Journal of High Energy Physics as doi:10.1007/JHEP03(2017)156.

1 Introduction

Measurement of the cross sections for inclusive jet production in proton-proton collisions is an ultimate test of quantum chromodynamics (QCD). The process $p + p \rightarrow \text{jet} + X$ probes the parton-parton interaction as described in perturbative QCD (pQCD), and is sensitive to the value of the strong coupling constant, α_S . Furthermore, it provides important constraints on the description of the proton structure, expressed by the parton distribution functions (PDFs).

In this analysis, the double-differential inclusive jet cross section is measured at the centre-of-mass energy $\sqrt{s} = 8 \text{ TeV}$ as a function of jet transverse momentum p_T and absolute jet rapidity $|y|$. Similar measurements have been carried out at the CERN LHC by the ATLAS and CMS Collaborations at 2.76 [1, 2] and 7 TeV [3–6], and by experiments at other hadron colliders [7–11].

The measured inclusive jet cross section at $\sqrt{s} = 7 \text{ TeV}$ is well described by pQCD calculations at next-to-leading order (NLO) at small $|y|$, but not at large $|y|$. The larger data sample at $\sqrt{s} = 8 \text{ TeV}$ allows QCD to be probed with higher precision extending the investigations to yet unexplored kinematic regions. In addition, the ratios of differential cross sections at different centre-of-mass energies can be determined. In Ref. [12] an increased sensitivity of such ratios to PDFs was suggested.

The data were collected with the CMS detector at the LHC during 2012 and correspond to an integrated luminosity of 19.7 fb^{-1} . The average number of multiple collisions within the same bunch crossing (known as pileup) is 21. A low-pileup data sample corresponding to an integrated luminosity of 5.6 pb^{-1} is collected with an average of four interactions per bunch crossing; this is used for a low- p_T jet cross section measurement. The measured cross sections are corrected for detector effects and compared to the QCD prediction at NLO. The high- p_T part of the differential cross section, where the sensitivity to the value of α_S is maximal, is measured more accurately than before. Also, the kinematic region of small p_T and large y is probed. The measured cross section is used to extract the value of the strong coupling constant at the Z boson mass scale, $\alpha_S(M_Z)$, and to study the scale dependence of α_S in a wider kinematic range than is accessible at $\sqrt{s} = 7 \text{ TeV}$. Further, the impact of the present measurements on PDFs is illustrated in a QCD analysis using the present measurements and the cross sections of deep-inelastic scattering (DIS) at HERA [13].

2 The CMS detector

The central feature of the CMS apparatus is a superconducting solenoid of 6 m internal diameter, providing a magnetic field of 3.8 T. Within the solenoid volume are a silicon pixel and strip tracker, a lead tungstate crystal electromagnetic calorimeter (ECAL), and a brass and scintillator hadron calorimeter (HCAL), each composed of a barrel and two endcap sections. Forward calorimeters extend the pseudorapidity (η) coverage [14] provided by the barrel and endcap detectors. Muons are measured in gas-ionization detectors embedded in the steel flux-return yoke outside the solenoid.

The silicon tracker measures charged particles within the pseudorapidity range $|\eta| < 2.5$. It consists of 1440 silicon pixel and 15 148 silicon strip detector modules. For non-isolated particles of $1 < p_T < 10 \text{ GeV}$ and $|\eta| < 1.4$, the track resolutions are typically 1.5% in p_T and 25–90 (45–150) μm in the transverse (longitudinal) impact parameter [15]. The ECAL consists of 75 848 lead tungstate crystals, which provide coverage in $|\eta| < 1.479$ in a barrel region (EB) and $1.479 < |\eta| < 3.0$ in two endcap regions (EE). A preshower detector consisting of two

planes of silicon sensors interleaved with a total of $3X_0$ of lead is located in front of the EE. In the region $|\eta| < 1.74$, the HCAL cells have widths of 0.087 in η and 0.087 radians in azimuth (ϕ). In the η - ϕ plane, and for $|\eta| < 1.48$, the HCAL cells map on to 5×5 arrays of ECAL crystals to form calorimeter towers projecting radially outwards from close to the nominal interaction point. For $|\eta| > 1.74$, the coverage of the towers increases progressively to a maximum of 0.174 in $\Delta\eta$ and $\Delta\phi$. The hadronic forward (HF) calorimeters consist of iron absorbers with embedded radiation-hard quartz fibres, located at 11.2 m from the interaction point on both sides of the experiment covering the region of $2.9 < |\eta| < 5.2$. Half of the HF fibres run over the full depth of the absorber, while the other half start at a depth of 22 cm from the front of the detector to allow for a separation between electromagnetic and hadronic showers. The η - ϕ tower segmentation of the HF calorimeters is 0.175×0.175 , except for η above 4.7, where the segmentation is 0.175×0.35 .

The first level of the CMS trigger system, composed of custom hardware processors, uses information from the calorimeters and muon detectors to select events in a fixed time interval of less than 4 μ s. The high-level trigger (HLT) processor farm further decreases the event rate from 100 kHz to around 400 Hz, before data storage. A more detailed description of the CMS detector, together with a definition of the coordinate system used and the relevant kinematic variables, can be found in Ref. [14].

3 Jet reconstruction and event selection

The high- p_T jet measurement is based on data sets collected with six single-jet triggers in the HLT system that require at least one jet in the event with jet $p_T > 40, 80, 140, 200, 260$, and 320 GeV, respectively. All triggers were prescaled during the 2012 data-taking period except the highest threshold trigger. The efficiency of each trigger is estimated using triggers with lower p_T thresholds, and each is found to exceed 99% above the nominal p_T threshold. The p_T thresholds of each trigger and the corresponding effective integrated luminosity are listed in Table 1. The jet p_T range, reconstructed in the offline analysis, where the trigger with the lowest p_T threshold becomes fully efficient is also shown. This analysis includes jets with $74 < p_T < 2500$ GeV.

Table 1: HLT trigger ranges and effective integrated luminosities used in the jet cross section measurement. The luminosity is known with a 2.6% uncertainty.

Trigger p_T threshold (GeV)	40	80	140	200	260	320
Offline analysis p_T range (GeV)	74–133	133–220	220–300	300–395	395–507	507–2500
Effective integrated luminosity (pb^{-1})	7.9×10^{-2}	2.12	55.7	2.61×10^2	1.06×10^3	1.97×10^4

Events for the low- p_T jet analysis are collected with a trigger that requires at least two charged tracks reconstructed in the pixel detector in coincidence with the nominal bunch crossing time. This selection is highly efficient for finding jets ($\simeq 100\%$) and also rejects noncollision background. The p_T range considered in the low- p_T jet analysis is 21–74 GeV.

The particle-flow (PF) event algorithm reconstructs and identifies each individual particle with an optimized combination of information from the various elements of the CMS detector [16, 17]. Selected events are required to have at least one reconstructed interaction vertex, and the primary interaction vertex (PV) is defined as the reconstructed vertex with the largest sum of

p_T^2 of its constituent tracks. The PV is required to be reconstructed from at least five tracks and to lie within 24 cm in the longitudinal direction from the nominal interaction point [15], and to be consistent with the measured transverse position of the beam. The energy of photons is obtained directly from the ECAL measurement and is corrected for zero-suppression effects. The energy of electrons is determined from a combination of the electron momentum at the PV as determined by the tracker, the energy of the corresponding ECAL cluster, and the energy sum of all bremsstrahlung photons spatially compatible with originating from the electron track. The transverse momentum of muons is obtained from the curvature of the corresponding track. The energy of charged hadrons is determined from a combination of their momentum measured in the tracker and the matching ECAL and HCAL energy deposits, corrected for zero-suppression effects and for the response function of the calorimeters to hadronic showers. Finally, the energy of neutral hadrons is obtained from the corresponding corrected ECAL and HCAL energies. In the forward region, the energies are measured in the HF detector.

For each event, hadronic jets are clustered from the reconstructed particles with the infrared and collinear safe anti- k_T algorithm [18], as implemented in the FASTJET package [19], with a size parameter R of 0.7. Jet momentum is determined as the vector sum of the momenta of all particles in the jet, and is found from simulation to be within 5% to 10% of the true momentum over the whole p_T spectrum and detector acceptance, before corrections are applied. In order to suppress the contamination from pileup, only reconstructed charged particles associated to the PV are used in jet clustering. Jet energy scale (JES) corrections are derived from simulation, by using events generated with PYTHIA6 and processed through the CMS detector simulation that is based on the GEANT 4 [20] package, and from in situ measurements by exploiting the energy balance in dijet, photon+jet, and Z+jet events [21, 22]. The PYTHIA6 version 4.22 [23] is used, with the Z2* tune. The Z2* tune is derived from the Z1 tune [24] but uses the CTEQ6L [25] parton distribution set whereas the Z1 tune uses the CTEQ5L set. The Z2* tune is the result of retuning the PYTHIA6 parameters PARP(82) and PARP(90) by means of the automated PROFESSOR tool [26], yielding PARP(82)=1.921 and PARP(90)=0.227. The JES corrections account for residual nonuniformities and nonlinearities in the detector response. An offset correction is required to account for the extra energy clustered into jets due to pileup. The JES correction, applied as a multiplicative factor to the jet four momentum vector, depends on the values of jet η and p_T . For a jet with a p_T of 100 GeV the typical correction is about 10%, and decreases with increasing p_T . The jet energy resolution (JER) is approximately 15% at 10 GeV, 8% at 100 GeV, and 4% at 1 TeV.

The missing transverse momentum vector, \vec{p}_T^{miss} , is defined as the projection on the plane perpendicular to the beams of the negative vector sum of the momenta of all reconstructed particles in an event. Its magnitude is referred to as E_T^{miss} . A requirement is made that the ratio of E_T^{miss} and the sum of the transverse energy of the PF particles is smaller than 0.3, which removes background events and leaves a negligible residual contamination. Additional selection criteria are applied to each event to remove spurious jet-like signatures originating from isolated noise patterns in certain HCAL regions. To suppress the noise patterns, tight identification criteria are applied: each jet should contain at least two PF particles, one of which is a charged hadron, and the jet energy fraction carried by neutral hadrons and photons should be less than 90%. These criteria have an efficiency greater than 99% for genuine jets. Events are selected that contain at least one jet with a p_T higher than the p_T threshold of the lowest-threshold trigger that recorded the event.

4 Measurement of the jet differential cross section

The double-differential inclusive jet cross section is defined as

$$\frac{d^2\sigma}{dp_T dy} = \frac{1}{\epsilon \mathcal{L}_{\text{int,eff}}} \frac{N_{\text{jets}}}{\Delta p_T (2\Delta|y|)}, \quad (1)$$

where N_{jets} is the number of jets in a kinematic interval (bin) of transverse momentum and rapidity, Δp_T and $\Delta|y|$, respectively; $\mathcal{L}_{\text{int,eff}}$ is the effective integrated luminosity contributing to the bin; ϵ is the product of the trigger and jet selection efficiencies, and is greater than 99%. The widths of the p_T bins increase with p_T and are proportional to the p_T resolution. The phase space in absolute rapidity $|y|$ is subdivided into six bins starting from $y = 0$ up to $|y| = 3.0$ with $\Delta|y| = 0.5$. In the low- p_T jet measurement an additional rapidity bin $3.2 < |y| < 4.7$ is included. The statistical uncertainty for each bin is computed according to the number of events contributing to at least one entry per event [6], corrected for possible multiple entries per event. This correction is small, since at least 90% of the observed jets in each Δp_T and $\Delta|y|$ bin originate from different events.

In order to compare the measured cross section with theoretical predictions at particle level, the steeply falling jet p_T spectra must be corrected for experimental p_T resolution. An unfolding procedure, based on the iterative D'Agostini method [27], implemented in the ROOUNFOLD package [28], is used to correct the measured spectra for detector effects. The response matrix is created by the convolution of theoretically predicted spectra, discussed in Section 5, with the JER effects. These effects are evaluated as a function of p_T with the CMS detector simulation, after correcting for the residual differences from data [21]. The unfolding procedure induces statistical correlations among the bins. The sizes of these correlations typically vary between 10% and 20%.

The dominant contribution to the experimental systematic uncertainty in the measured cross section is from the JES corrections, determined as in Ref. [21, 22]. For the high- p_T jet data set, this uncertainty is decomposed into 24 independent sources, corresponding to the different components of the corrections: pileup effects, relative calibration of JES versus η , absolute JES including p_T dependence, and differences in quark- and gluon-initiated jets. The set of components, used here, is discussed in detail in Ref. [22], and represents an evolution of the decomposition presented in Ref. [29]. The low-pileup data set uses a reduced number of components, since the pileup-related corrections are negligible, and there is no JES time dependence. Moreover, the central values of the corrections, for the components common between the two data sets, are not the same; the low- p_T jet analysis uses corrections computed only on the initial part of the 2012 data sample. The impact of the uncertainty induced by each correction component on the measured cross section is evaluated separately. The JES-induced uncertainty in the cross section depends on p_T and y . For the high- p_T data, this ranges from 2% to 4% in the sub-TeV region at central rapidity to about 20% in the highest p_T bins for rapidities $1.0 < |y| < 2.0$. Due to the different set of corrections used, the low- p_T jet cross section has a larger JES uncertainty than the contiguous bins of the high- p_T part, and this effect becomes more pronounced as the jet rapidity increases.

To account for the residual effects of small inefficiencies of less than 1% in the trigger performances and jet identification, an uncertainty of 1%, uncorrelated across all jet p_T and y bins, is assigned to each bin.

The unfolding procedure is affected by the uncertainties in the JER parameterization, which are derived from the simulation. The JER parameters are varied by one standard deviation up and down, and the corresponding response matrices are used to unfold the measured spectra.

The JER-induced uncertainty amounts to 1–5% in the high- p_T jet region, but can exceed 30% in the low- p_T jet region.

The uncertainties in the integrated luminosity, which propagate directly to the cross section, are 2.6% [30] and 4.4% [31] for normal and low-pileup data samples, respectively. Other sources of uncertainty, such as the jet angular resolution and the model dependence of the unfolding, arise from the theoretical p_T spectrum used to calculate the response matrix and have less than 1% effect on the cross section. The total experimental systematic uncertainty in the measured cross section is obtained as a quadratic sum of contributions due to uncertainties in JES, JER, and integrated luminosity.

5 Theoretical predictions

Theoretical predictions for the jet cross section are known at NLO accuracy in pQCD [32, 33], and the NLO electroweak corrections have been computed in Ref. [34]. The pQCD NLO calculations are performed by using the NLOJET++ (version 4.1.3) program [32, 33] as implemented in the FASTNLO (version 2.1) package [35]. The renormalization (μ_R) and factorization (μ_F) scales are both set to the leading jet p_T . The calculations are performed by using six PDF sets determined at NLO: CT10 [36], MSTW2008 [37], NNPDF2.1 [38], NNPDF3.0 [39], HERAPDF1.5 [40], and ABM11 [41]. Each PDF set is available for a range of $\alpha_S(M_Z)$ values. The number of active (massless) flavours chosen in NLOJET++ is five in all of the PDF sets except NNPDF2.1, where it is set to six. All the PDF sets use a variable flavour number scheme, except ABM11, which uses a fixed flavour number scheme. The basic characteristics of each PDF set are summarized in Table 2.

Table 2: The PDF sets used in comparisons to the data together with the corresponding number of active flavours N_f , the assumed masses M_t and M_Z of the top quark and Z boson, the default values of the strong coupling constant $\alpha_S(M_Z)$, and the ranges in $\alpha_S(M_Z)$ available for fits. For CT10 the updated versions of 2012 are used.

PDF set	Refs.	Order	N_f	M_t (GeV)	M_Z (GeV)	$\alpha_S(M_Z)$	$\alpha_S(M_Z)$ range
ABM11	[41]	NLO	5	180	91.174	0.1180	0.110–0.130
CT10	[36]	NLO	≤ 5	172	91.188	0.1180	0.112–0.127
HERAPDF1.5	[40]	NLO	≤ 5	180	91.187	0.1176	0.114–0.122
MSTW2008	[37]	NLO	≤ 5	10^{10}	91.1876	0.1202	0.110–0.130
NNPDF2.1	[38]	NLO	≤ 6	175	91.2	0.1190	0.114–0.124
NNPDF3.0	[39]	NLO	≤ 5	175	91.2	0.1180	0.115–0.121

The parton-level calculation at NLO has to be supplemented with corrections due to nonperturbative (NP) effects, i.e. hadronization and multiparton interactions (MPI). The nonperturbative effects are estimated using both leading order (LO) and NLO event generators. In the former case, the correction is evaluated by averaging those provided by PYTHIA6 [23] (version 4.26), using tune Z2*, and HERWIG++ (version 2.4.2) [42], using tune UE [43]. The size of these corrections ranges from 20% at low p_T to 1% at the highest p_T of 2.5 TeV. The NLO nonperturbative correction is derived using POWHEG [44–47], interfaced with PYTHIA6 for parton shower, MPI, and hadronization. The nonperturbative correction factors are derived in this case by averaging the results for two different tunes of PYTHIA6, Z2* and P11 [48]. Hadronization models have been tuned by using LO calculations for the hard scattering, and applying these tunes to NLO-based calculations is not expected to provide optimal results. On the other hand, the

application of nonperturbative corrections based on LO calculations to NLO predictions implicitly assumes that the behaviour of nonperturbative effects is independent of the hard scattering description. To take into account both facts, the final number used for the nonperturbative correction, C^{NP} , is an arithmetic average of the LO- and NLO-based estimates. Half the width of the envelope of these predictions is used as the uncertainty due to the nonperturbative correction. Figure 1 shows the nonperturbative correction factors derived by combining both LO- and NLO-based calculations.

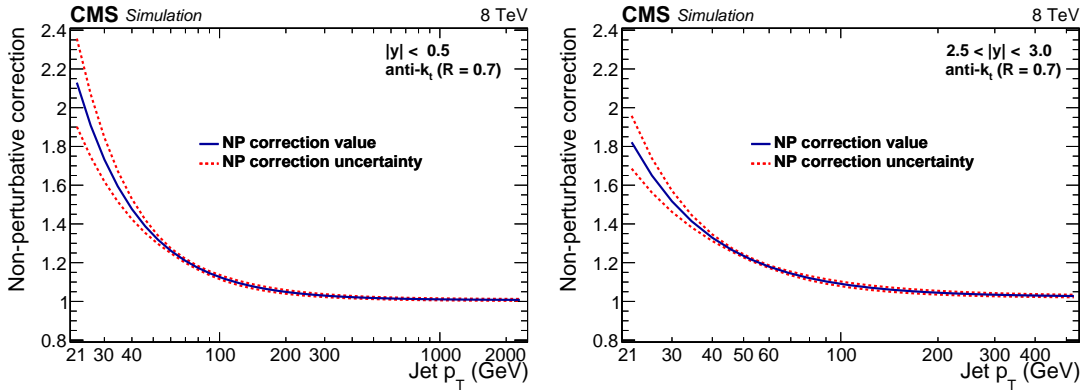


Figure 1: The nonperturbative correction factor shown for the central (left) and outermost (right) absolute rapidity bins as a function of jet p_T . The correction is obtained by averaging LO- and NLO-based predictions, and the envelope of these predictions is used as the uncertainty band.

The uncertainty in the NLO pQCD calculation arising from missing higher-order corrections is estimated by varying the renormalization and factorization scales in the following six combinations of scale factors: $(\mu_R/\mu, \mu_F/\mu) = (0.5, 0.5), (2, 2), (1, 0.5), (1, 2), (0.5, 1), (2, 1)$, where μ is the default choice equal to the jet p_T , and considering the largest variation in the prediction as the uncertainty. The uncertainty related to the choice of scale ranges from 5% to 10% for $|y| < 1.5$ and increases to 40% for the outer $|y|$ bins and for high p_T . The PDF uncertainties are estimated following the prescription from each PDF group by using the provided eigenvectors (or replicas in case of NNPDF). The corresponding uncertainty in the predicted cross section varies from 5% to 30% in the entire p_T range for $|y| \leq 1.5$. Beyond $|y| = 1.5$, in the outer rapidity region, these uncertainties become as large as 50% at high p_T and even increase up to 100% for the CT10 and HERAPDF1.5 sets. The nonperturbative correction induces an additional uncertainty, which is estimated in the central rapidity bin to range between 1.4% at $p_T \sim 100$ GeV to 0.06% at ~ 2.5 TeV. Overall, the PDF uncertainty is dominant.

Electroweak effects, which arise from the virtual exchange of the massive W and Z gauge bosons, induce corrections with magnitudes given by the Sudakov logarithmic factor $\alpha_W \ln^2(Q^2/M_W^2)$, where α_W is the weak coupling constant, M_W is the mass of the W boson, and Q is the energy scale of the interaction. For high- p_T jets, the values of the logarithm, and therefore the correction, become large. The derivation of the electroweak correction factor, applied to the NLO pQCD spectrum corrected for nonperturbative effects, is provided in Ref. [34]. Figure 2 shows the electroweak correction for the two extreme rapidity regions as a function of jet p_T . In the most central rapidity bin for the high- p_T region, the correction factor is as large as 14%. Electroweak corrections are not applied to the low- p_T results, where they are negligible.

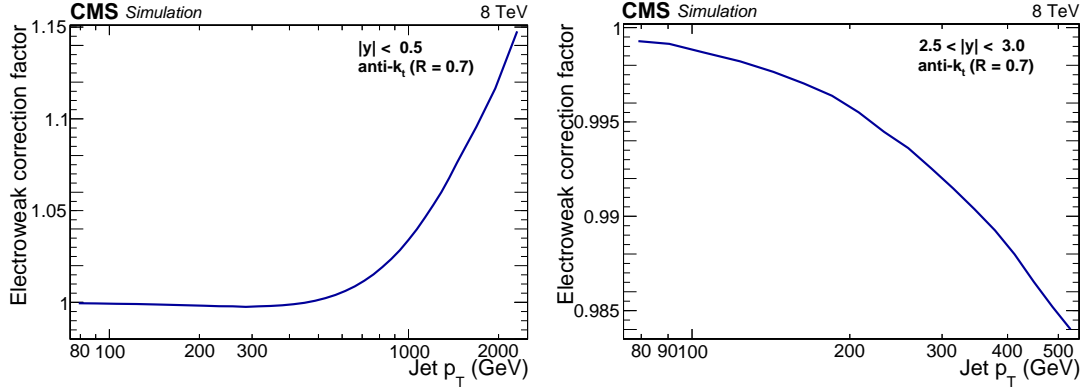


Figure 2: Electroweak correction factor for the central (left) and outermost (right) rapidity bins as a function of jet p_T .

6 Comparison of theory and data

The measured double-differential cross sections for inclusive jet production are shown in Fig. 3 as a function of p_T in the various $|y|$ ranges after unfolding the detector effects. This measurement is compared with the theoretical prediction discussed in Section 5 using the CT10 PDF set. The ratios of the data to the theoretical predictions in the various $|y|$ ranges are shown for the CT10 PDF set in Fig. 4. Good agreement is observed for the entire kinematic range with some exceptions in the low- p_T region.

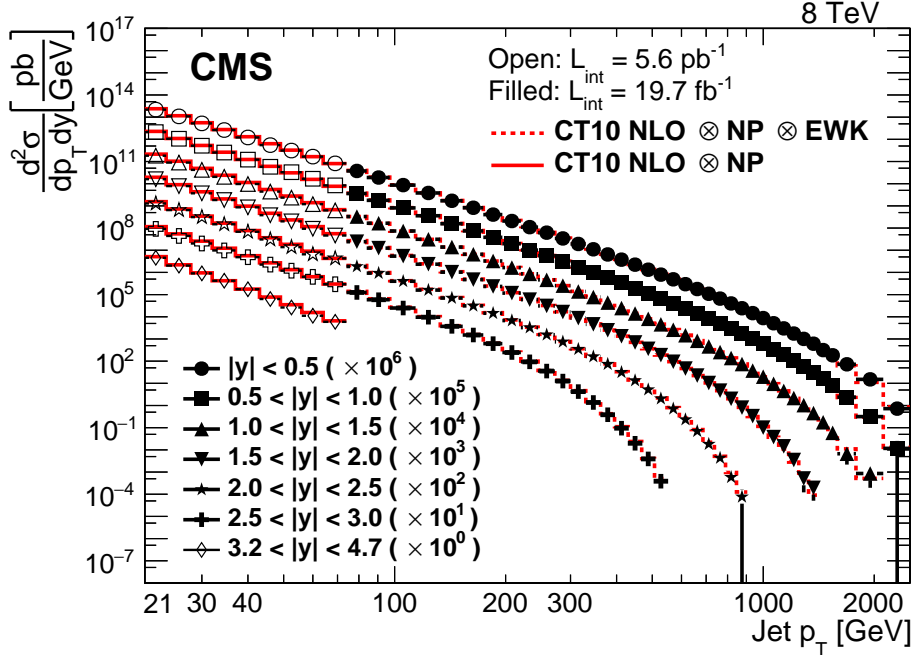


Figure 3: Double-differential inclusive jet cross sections as function of jet p_T . Data (open points for the low- p_T analysis, filled points for the high- p_T one) and NLO predictions based on the CT10 PDF set corrected for the nonperturbative factor for the low- p_T data (solid line) and the nonperturbative and electroweak correction factors for the high- p_T data (dashed line). The comparison is carried out for six different $|y|$ bins at an interval of $\Delta|y| = 0.5$.

Figure 5 presents the ratios of the measurements and a number of theoretical predictions based on alternative PDF sets to the CT10 based prediction. A χ^2 value is computed based on the measurements, their covariance matrices, and the theoretical predictions, as described in detail

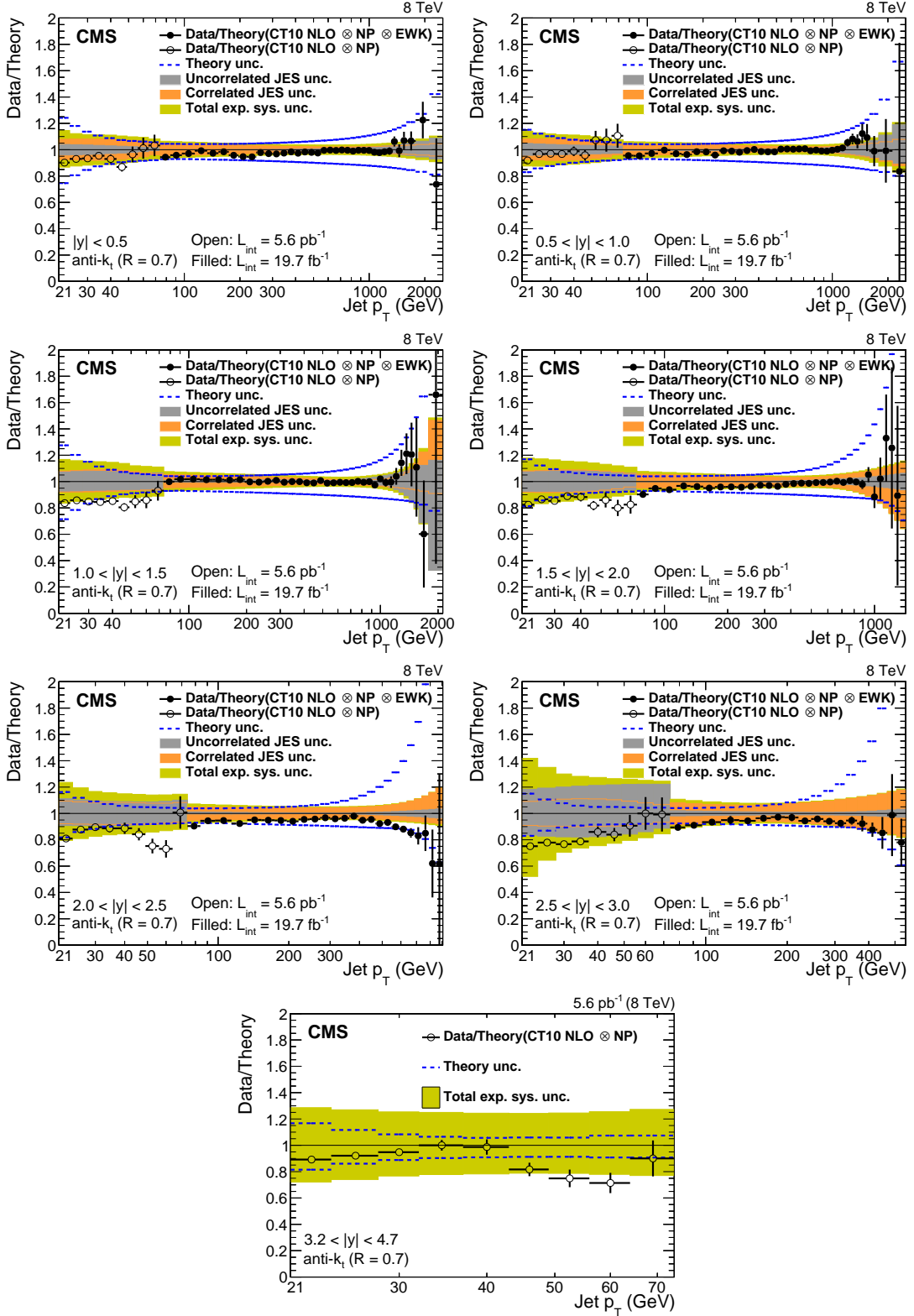


Figure 4: Ratios of data to the theory prediction using the CT10 PDF set. For comparison, the total theoretical (band enclosed by dashed lines) and the total experimental systematic uncertainties (band enclosed by full lines) are shown as well. The error bars correspond to the statistical uncertainty in the data.

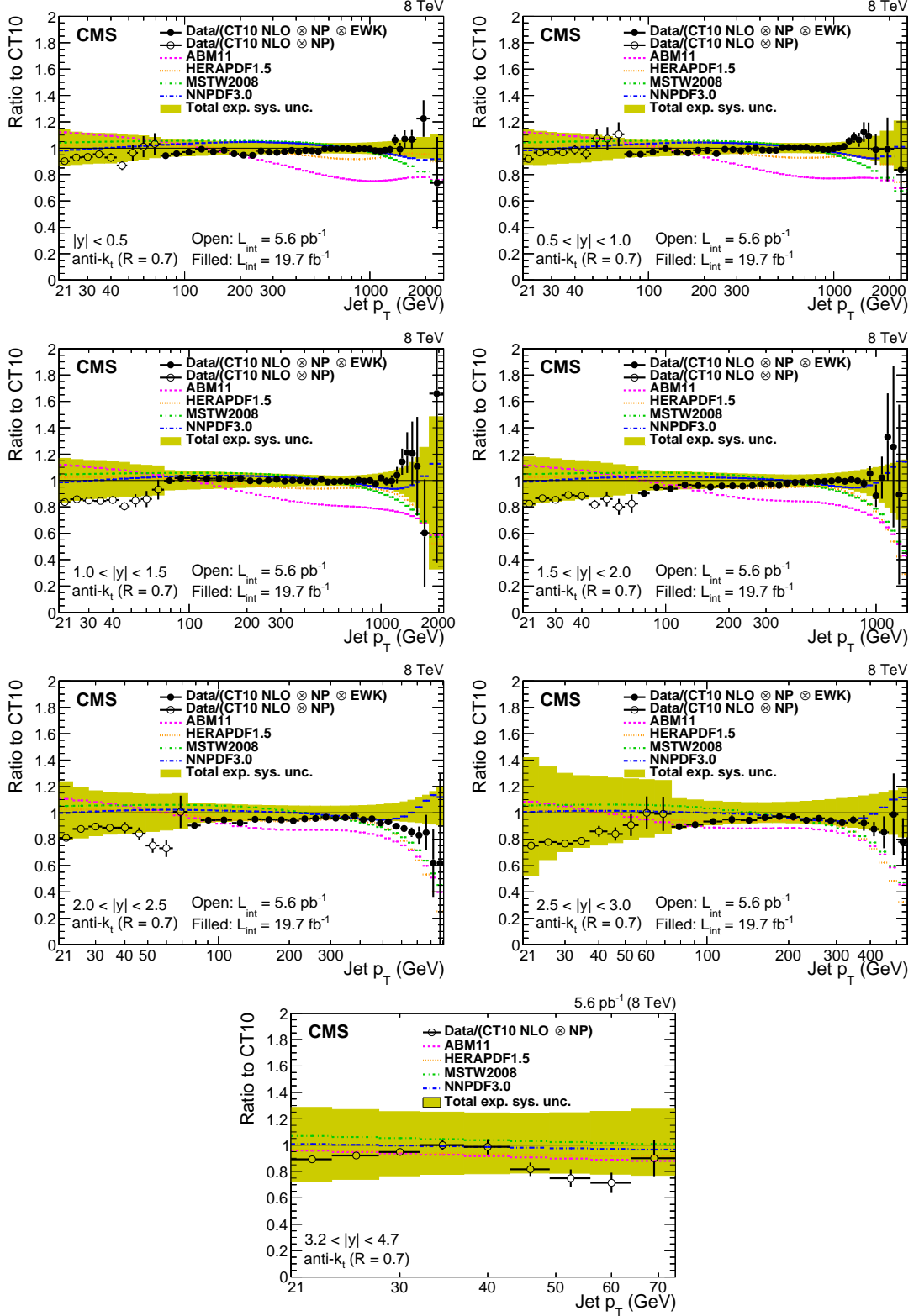


Figure 5: Ratios of data and alternative predictions to the theory prediction using the CT10 PDF set. For comparison, predictions employing five other PDF sets are shown in addition to the total experimental systematic uncertainties (band enclosed by full lines). The error bars correspond to the statistical uncertainty in the data.

in Section 8. The values for χ^2 for the comparison between data and theory based on different PDF sets for the high- p_T region are summarized in Table 3.

Table 3: Summary of the χ^2 values for the comparison of data and theoretical predictions based on different PDF sets in each $|y|$ range, where cross sections are measured for a number of p_T bins N_{bins} .

$ y $	N_{bins}	CT10	HERAPDF1.5	MSTW2008	NNPDF2.1	ABM11	NNPDF3.0
0.0–0.5	37	49.2	66.3	68.0	58.3	136.6	62.5
0.5–1.0	37	28.7	47.2	39.0	35.4	155.5	42.2
1.0–1.5	36	19.3	28.6	27.4	20.2	111.8	25.9
1.5–2.0	32	65.7	49.0	55.3	54.5	168.1	64.7
2.0–2.5	25	38.7	32.0	53.1	34.6	80.2	36.0
2.5–3.0	18	14.5	19.1	18.2	15.4	43.8	16.3

In most cases the theoretical predictions agree with the measurements. The exception is the ABM11 PDF set, where significant discrepancies are visible. Significant differences between the theoretical predictions obtained by using different PDF sets are observed in the high- p_T range. The predictions based on CT10 PDF show the best agreement with data, quantified by the lowest χ^2 for most rapidity ranges, while predictions using MSTW, ABM11, and HERAPDF1.5 exhibit differences compared to data and to the prediction based on CT10, exceeding 100% in the highest p_T range.

In the transition between the low- and high- p_T jet regions, some discontinuity can be observed in the measured values, although they are generally compatible within the total experimental uncertainties. The highest p_T bins of the low- p_T jet range suffer from a reduced sample size, and therefore have a statistical uncertainty significantly larger than the first bin of the high- p_T jet region. The JES corrections for the low- and high- p_T regions are different, in particular in the p_T -dependent components, and this also contributes to the observed fluctuations in the matching region. The corresponding uncertainties are treated as uncorrelated between the low- and high- p_T regions. The overall estimated systematic uncertainties account for these residual effects. The transition region between the low- and high- p_T jet measurements has limited sensitivity to α_S and no impact in constraining PDFs, since it probes the x -range where the PDFs are well constrained by more precise DIS data.

7 Ratios of cross sections measured at different \sqrt{s} values

Ratios of cross sections measured at different energies may show a better sensitivity to PDFs than cross sections at a single energy, provided that the contributions to the theoretical and experimental uncertainties from sources other than the PDFs themselves are reduced. A calculation of the ratio of cross sections measured at 7 and 8 TeV presented in Ref. [12], for instance, suggests a larger sensitivity to PDFs in the jet p_T range between 1 and 2 TeV. Therefore, it is interesting to study such cross section ratios.

Differential cross sections for the inclusive jet production have been measured by the CMS Collaboration at $\sqrt{s} = 2.76$ [2] and 7 TeV [6]. Ratios are computed of the double-differential cross section presented in this paper at 8 TeV to the corresponding measurements at different energies. For $p_T > 74$ GeV, the choice of jet p_T and rapidity bins is identical for the various measurements, thus allowing an easy computation of the ratio. Only the high- p_T jet data set at 8 TeV is used, since no counterpart of the low- p_T jet analysis is available for the other centre-of-mass energies.

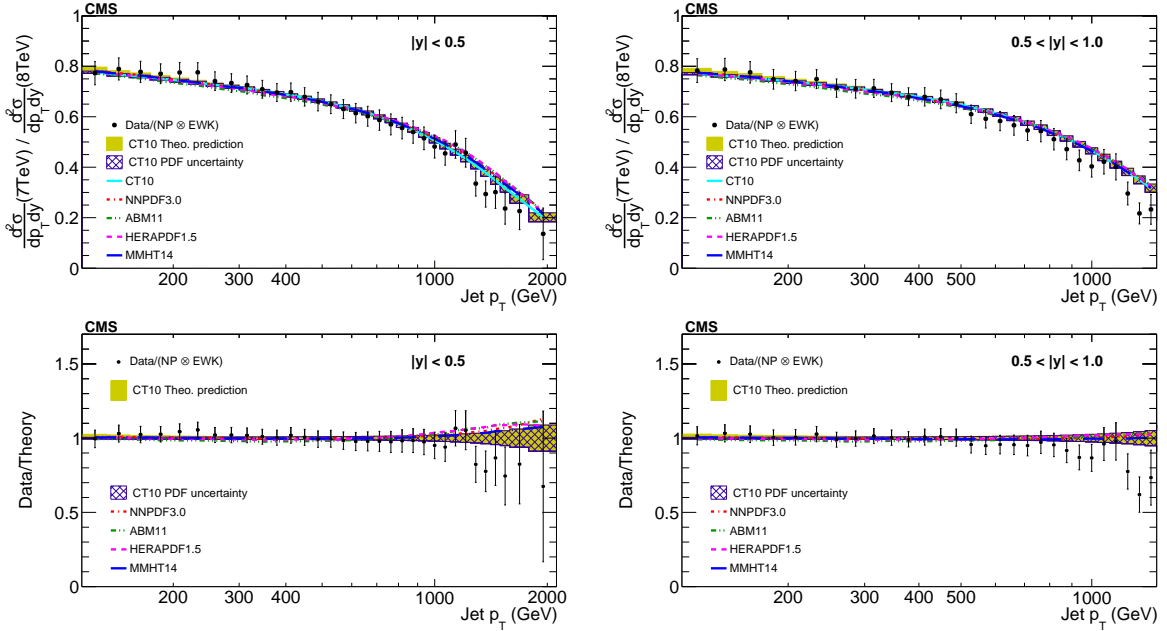


Figure 6: The ratios (top panels) of the inclusive jet production cross sections at $\sqrt{s} = 7$ and 8 TeV , shown as a function of jet p_T for the absolute rapidity $|y| < 0.5$ (left) and $0.5 < |y| < 1.0$ (right). The data (closed symbols) are shown with total uncertainties (vertical error bars). The NLO pQCD prediction using the CT10 PDF is shown with its total uncertainty (shaded band) and the contribution of the PDF uncertainty (hatched band). Predictions obtained using alternative PDF sets are shown by lines of different styles without uncertainties. The data to theory ratios (bottom panels) are shown by using the same notations for the respective rapidities. The last bin for the $|y| < 0.5$ region is wider than the others in order to reduce the statistical uncertainty.

As a result of partial cancellation of the systematic uncertainties, the relative precision of the ratios is improved compared with the cross section. Experimental correlations between the measurements at different centre-of-mass energies are taken into account in the computation of the total experimental uncertainty. As a consequence of the unfolding procedure, the results of the cross section measurements at each energy are statistically correlated between different bins, while the measurements at different energies are not statistically correlated with each other. The statistical uncertainties in the ratio measurement are calculated by using linear error propagation, taking into account the bin-to-bin correlations in the unfolded data. Correlations between the components of the jet energy corrections at different energies are included, as well as correlations in JER. Uncertainties related to the determination of luminosity are assumed to be uncorrelated.

The theoretical uncertainties are approached in a similar manner: the uncertainties in nonperturbative corrections, PDFs, and those arising due to scale variations are assumed to be fully correlated.

The ratios of the cross sections measured at $\sqrt{s} = 7$ and 8 TeV are shown in Figs. 6–7 for the various rapidity bins and they are compared with theoretical predictions obtained using different PDF sets. A general agreement between data and theoretical predictions is observed. Some discrepancies are visible at high p_T , in particular in the $1.0 < |y| < 1.5$ range. In the cross section ratio the central values of the predictions are not strongly influenced by the choice of the PDFs. However, the uncertainty is mostly dominated by PDF uncertainties, which are represented here for CT10. The experimental uncertainty in the ratio is considerably larger than

the theoretical uncertainty. Consequently, no significant constraints on PDFs can be expected from the inclusive jet cross section ratio of 7 to 8 TeV.

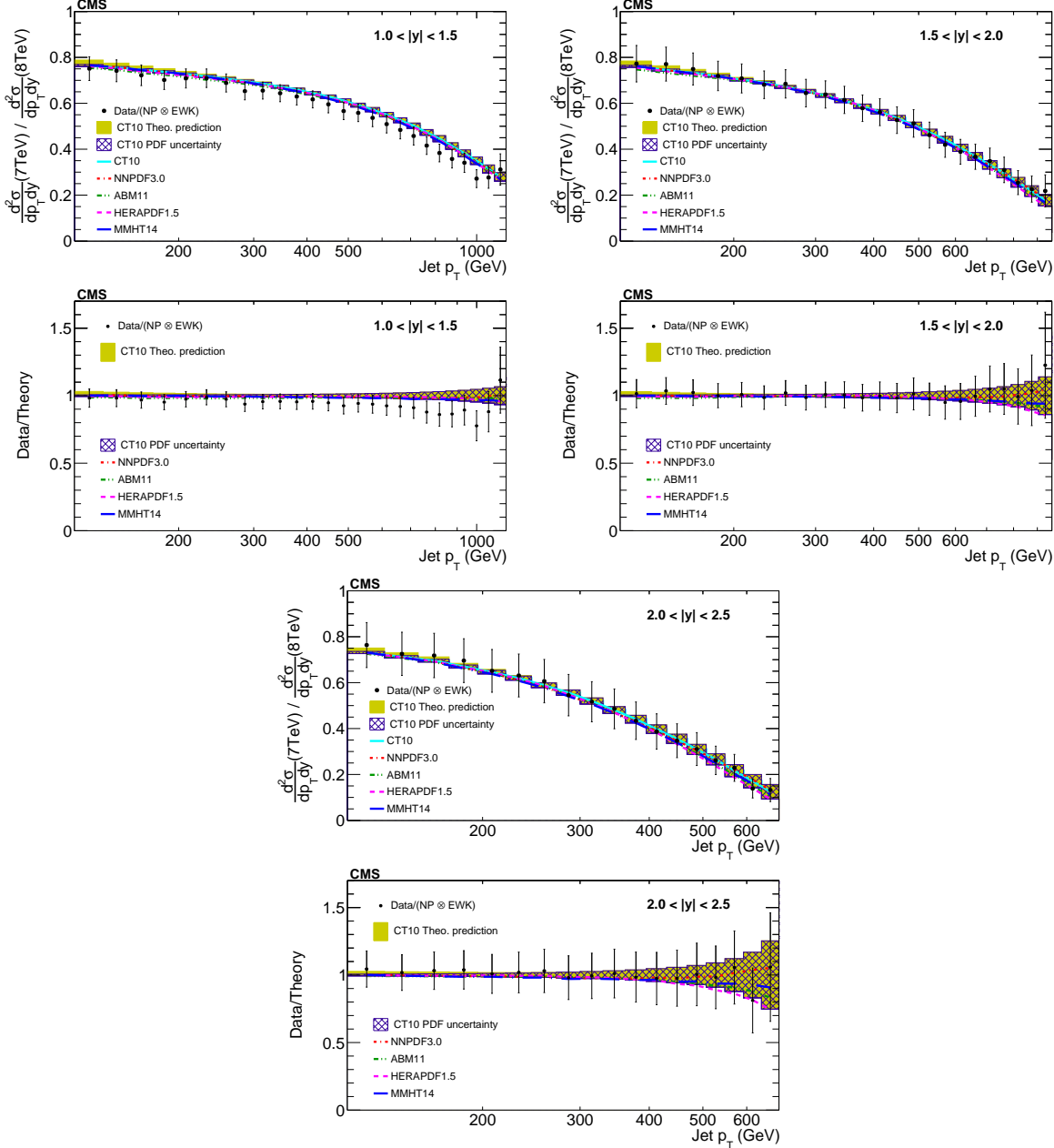


Figure 7: The ratios of the inclusive jet production cross sections at $\sqrt{s} = 7$ and 8 TeV shown as a function of jet p_T for the absolute rapidity $1.0 < |y| < 1.5$ (top left), $1.5 < |y| < 2.0$ (top right) and $2.0 < |y| < 2.5$ (bottom).

The ratios of the cross sections measured at 2.76 TeV to those measured at 8 TeV are determined in a similar way. Results are presented in Figs. 8–10, and compared to theoretical predictions that use different PDF sets. In general, the predictions describe the data well. The central value of the theoretical prediction and its uncertainty are completely dominated by the choice of and the uncertainty in the PDFs, demonstrating the strong sensitivity of the 2.76 to 8 TeV cross section ratio to the description of the proton structure.

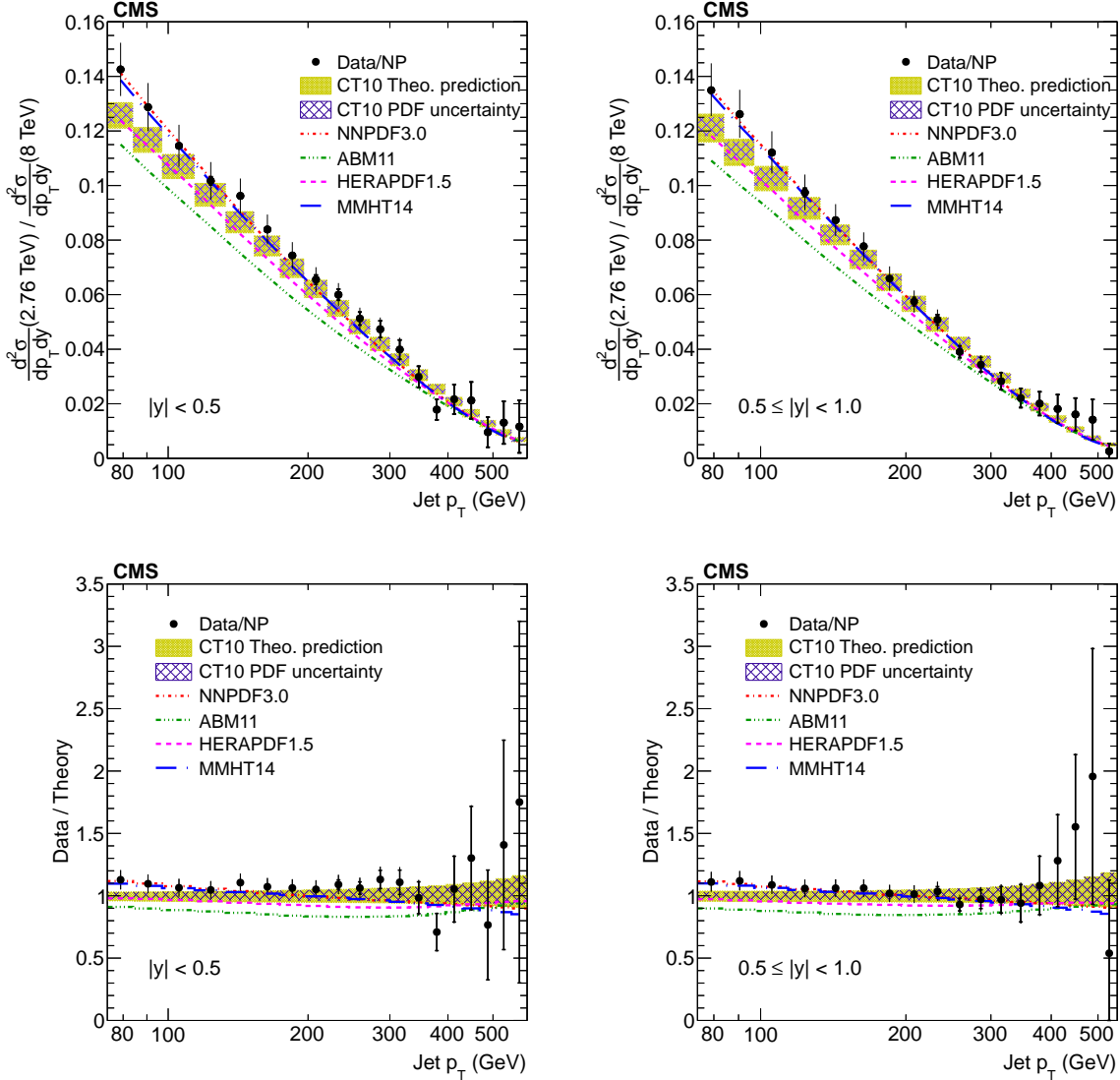


Figure 8: The ratios (top panels) of the inclusive jet production cross sections at $\sqrt{s} = 2.76$ and 8 TeV are shown as a function of jet p_T for the absolute rapidity range $|y| < 0.5$ (left) and $0.5 < |y| < 1.0$ (right). The data (closed symbols) are shown with their statistical (inner error bar) and total (outer error bar) uncertainties. For comparison, the NLO pQCD prediction by using the CT10 PDF is shown with its total uncertainty (light shaded band), while the contribution of the PDF uncertainty is presented by the hatched band. Predictions that use alternative PDF sets are shown by lines of different styles without uncertainties. The data to theory ratios (bottom panels) are shown using the same notations for the respective absolute rapidity ranges.

8 Determination of α_S

Measurements of jet production at hadron colliders can be used to determine the strong coupling constant α_S , as has been previously from the CMS 7 TeV inclusive jet measurement [29], and from Tevatron measurements [49–51]. The procedure to extract α_S in Ref. [29] is adopted here. Only the high- p_T jet data are used, since the sensitivity of the α_S predictions increases with jet p_T . The determination of α_S is performed by minimizing the χ^2 between the data and the theory prediction. The NLO theory prediction, corrected for nonperturbative and electroweak effects, is used. At NLO, the dependence of the differential inclusive jet production

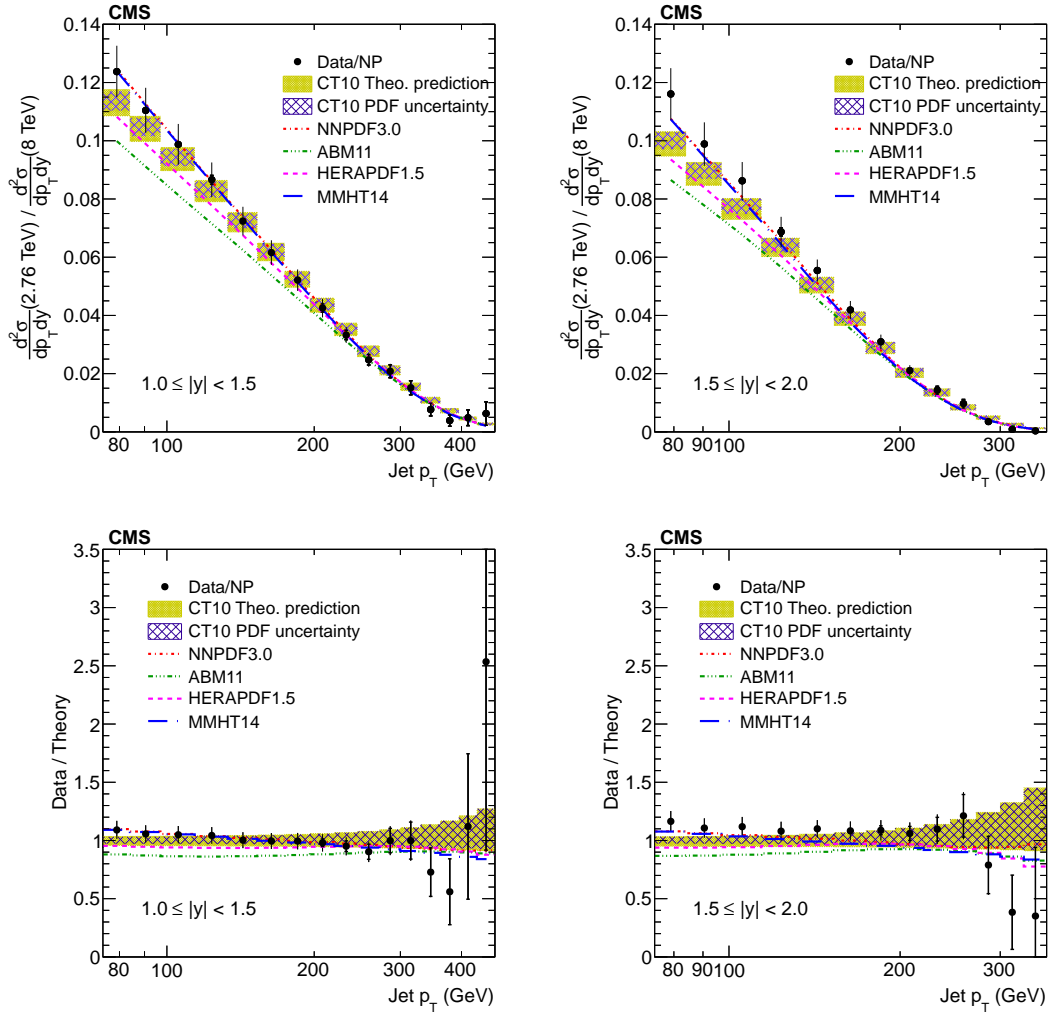


Figure 9: The ratios of the inclusive jet production cross sections at $\sqrt{s} = 2.76$ and 8 TeV shown as a function of jet p_T for the absolute rapidity ranges $1.0 < |y| < 1.5$ and $1.5 < |y| < 2.0$.

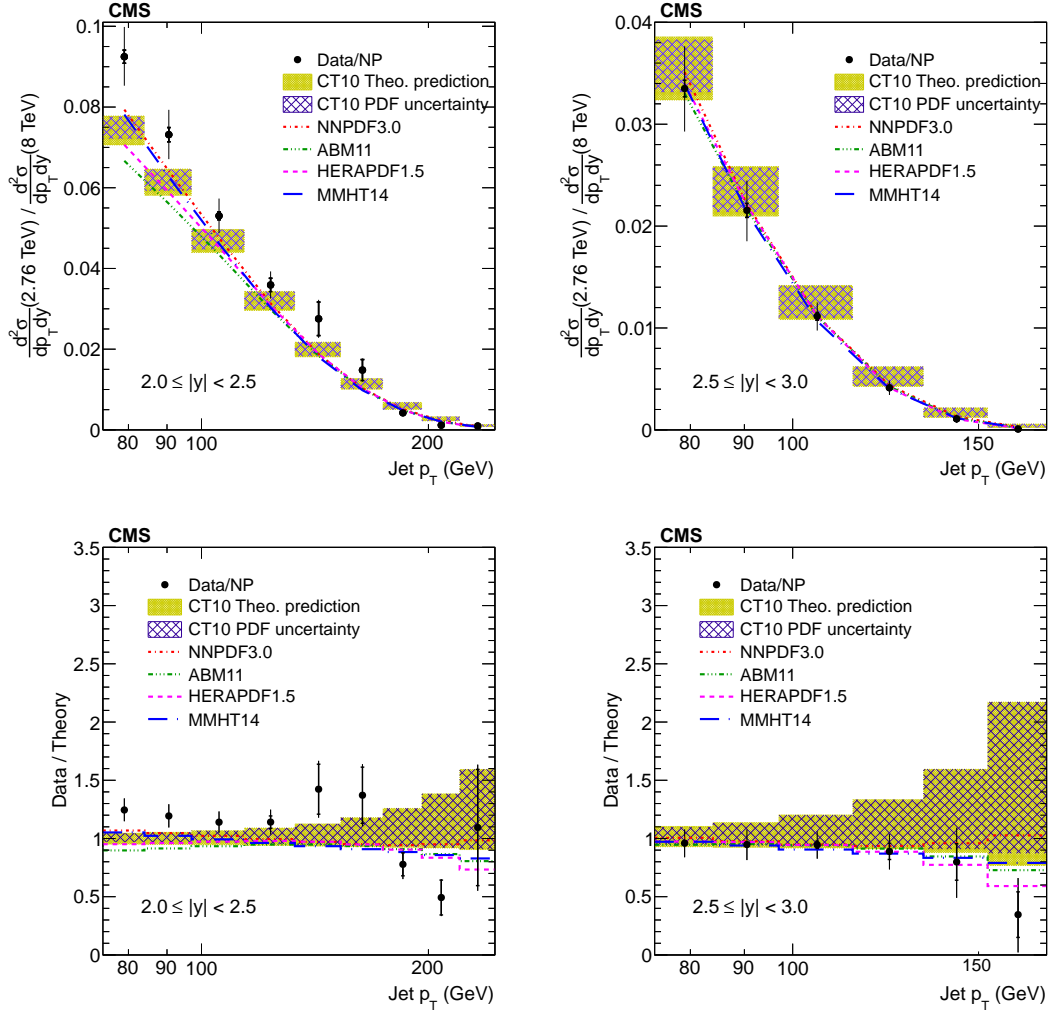


Figure 10: The ratios of the inclusive jet production cross sections at $\sqrt{s} = 2.76$ and 8 TeV shown as a function of jet p_T for the absolute rapidity ranges $2.0 < |y| < 2.5$ and $2.5 < |y| < 3.0$.

cross section $d\sigma/dp_T$ on α_S is given by:

$$\frac{d\sigma}{dp_T} = \alpha_S^2(\mu_R) \hat{X}^{(0)}(\mu_F, p_T) [1 + \alpha_S(\mu_R) K1(\mu_R, \mu_F, p_T)], \quad (2)$$

where α_S is the strong coupling, $\hat{X}^{(0)}(\mu_F, p_T)$ represents the LO contribution to the cross section and $K1(\mu_R, \mu_F, p_T)$ is an NLO correction term. A comparison with the measured spectrum gives an estimate of the input value of α_S for which the cross section, predicted from theory, has the best agreement with data.

The extraction of α_S is performed by a least squares minimization of the function

$$\chi^2(\alpha_S(M_Z)) = \left(D - T(\alpha_S(M_Z)) \right)^T C^{-1} \left(D - T(\alpha_S(M_Z)) \right), \quad (3)$$

where D is the array of measured values of the double-differential inclusive jet cross section for the different bins in p_T and $|y|$, $T(\alpha_S(M_Z))$ is the corresponding set of theoretical cross sections for a given value of $\alpha_S(M_Z)$, and C is the covariance matrix including all the experimental and theoretical uncertainties involved in the measurement. The total covariance matrix C is built from the individual components as follows:

$$C = C^{\text{stat}} + C^{\text{unfolding}} + \sum C^{\text{JES}} + C^{\text{uncor}} + C^{\text{lumi}} + C^{\text{PDF}} + C^{\text{NP}}, \quad (4)$$

where:

- C^{stat} is the statistical covariance matrix, taking into account the correlation between different p_T bins of the same rapidity range due to unfolding. Different rapidity ranges are considered as uncorrelated among themselves;
- $C^{\text{unfolding}}$ includes the uncertainty induced by the JER parameterization in the unfolding procedure;
- C^{JES} includes the uncertainty due to JES uncertainties, obtained as the sum of 24 independent matrices, one for each source of uncertainty;
- C^{uncor} includes all uncorrelated systematic uncertainties such as trigger and jet identification inefficiencies, and time dependence of the jet p_T resolution;
- C^{lumi} includes the 2.6% luminosity uncertainty;
- C^{PDF} is related to uncertainties in the PDF used in the theoretical prediction;
- C^{NP} includes the uncertainty due to nonperturbative corrections in the theoretical prediction.

The unfolding, JES, lumi, PDF, and NP systematic uncertainties are considered as 100% correlated among all p_T and $|y|$ bins.

The extraction of α_S uses the CT10 NLO PDF set in the theoretical calculation, since it provides the best agreement with measured cross sections, as shown in Section 6. This PDF set provides variants corresponding to 16 different $\alpha_S(M_Z)$ values in the range 0.112–0.127 in steps of 0.001. The sensitivity of the theory prediction to the α_S choice in the PDF is illustrated in Fig. 11.

The χ^2 in Eq. (3) is computed, combining all p_T and $|y|$ intervals, for each of the variants corresponding to a different α_S value, as shown in Fig. 12. The variation of χ^2 with α_S is fitted with a fourth-order polynomial, and the minimum (χ^2_{min}) corresponds to the best $\alpha_S(M_Z)$ value. Uncertainties are determined using the $\Delta\chi^2 = 1$ criterion. The individual contribution from each uncertainty source listed in Eq. (4) is estimated as the quadratic difference between the

main result and the result of an alternative fit, in which that particular source is left out of the covariance matrix definition.

The uncertainties due to the choice of the renormalization and factorization scales are evaluated by variations of the default μ_R , μ_F values, set to jet p_T , in the following six combinations: $(\mu_R / p_T, \mu_F / p_T) = (0.5, 0.5), (0.5, 1), (1, 0.5), (1, 2), (2, 1)$, and $(2, 2)$. The χ^2 minimization with respect

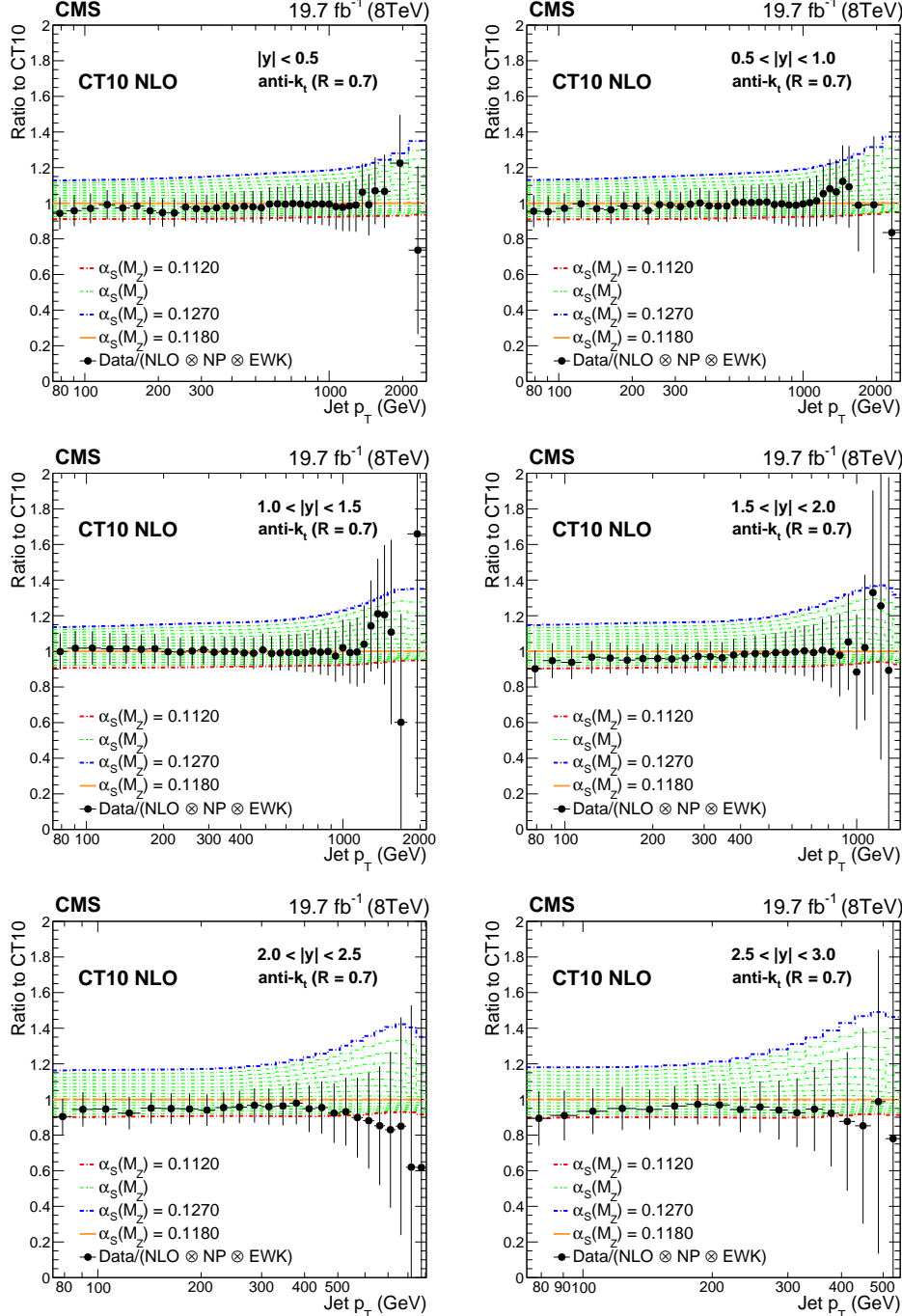


Figure 11: Ratio of data over theory prediction (closed circles) using the CT10 NLO PDF set, with the default $\alpha_S(M_Z)$ value of 0.118. Dashed lines represent the ratios of the predictions obtained with the CT10 PDF set evaluated with different $\alpha_S(M_Z)$ values, to the central one. The error bars correspond to the total uncertainty of the data.

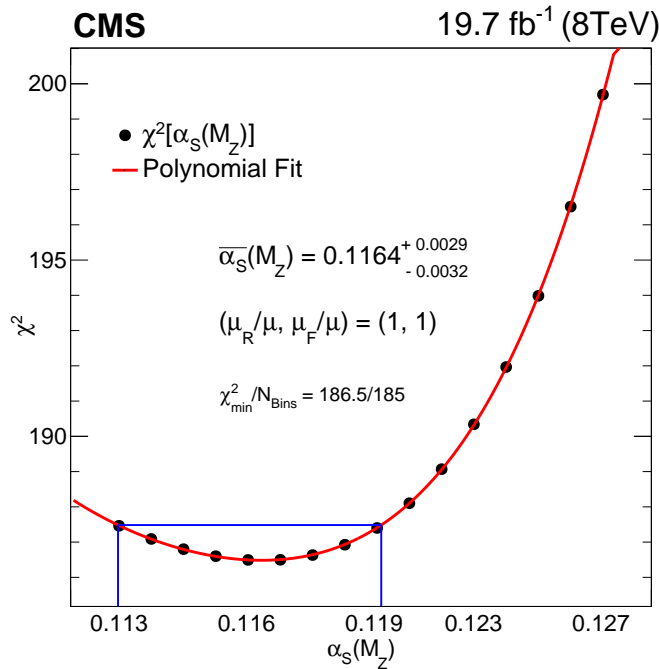


Figure 12: The χ^2 minimization with respect to $\alpha_S(M_Z)$ by using the CT10 NLO PDF set and data from all rapidity bins. The uncertainty is obtained from the $\alpha_S(M_Z)$ values for which χ^2 is increased by one with respect to the minimum value, indicated by the box. The curve corresponds to a fourth-degree polynomial fit through the available χ^2 points.

to $\alpha_S(M_Z)$ is repeated in each case, and the maximal upwards and downwards deviations of $\alpha_S(M_Z)$ from the central result are taken as the corresponding uncertainties.

In Table 4, the fitted values of α_S are presented for each rapidity bin, separately, and for the whole range. The contribution to the uncertainty due to each individual source is also given, together with the best χ^2_{min} value for each separate fit. The largest source of uncertainty in the determination of α_S is due to the choice of renormalization and factorization scales, pointing to the need for including higher order corrections in the theoretical calculations.

The best value obtained, by using the CT10 NLO PDF set, is

$$\alpha_S(M_Z)(\text{NLO}) = 0.1164^{+0.0025}_{-0.0029}(\text{PDF})^{+0.0053}_{-0.0028}(\text{scale}) \pm 0.0001(\text{NP})^{+0.0014}_{-0.0015}(\text{exp}) = 0.1164^{+0.0060}_{-0.0043}.$$

Alternatively, the value of $\alpha_S(M_Z)$ is also determined using the NNPDF3.0 NLO PDF, resulting in $\alpha_S(M_Z) = 0.1172^{+0.0083}_{-0.0075}$. These values of $\alpha_S(M_Z)$ are compatible with the current world average $\alpha_S(M_Z) = 0.1181 \pm 0.0011$ [52].

The value of α_S depends on the scale Q at which it is evaluated, decreasing as Q increases. The measured p_T interval 74–2500 GeV is divided into nine different ranges as shown in the first column in Table 5, and $\alpha_S(M_Z)$ is determined for each of them.

The Q scale corresponding to each p_T range is evaluated as the cross section weighted average p_T for that range. The extracted $\alpha_S(M_Z)$ values are evolved to the Q scale corresponding to the range, using the 2-loop 5-flavour renormalization group (RG) evolution equation, resulting in the $\alpha_S(Q)$ values listed in Table 5. The same RG equation is used to obtain the corresponding uncertainties. The contributions to both the experimental and theoretical uncertainties are shown in Table 6. A comparison of these results with those from the CMS [53–55],

Table 4: Results for $\alpha_S(M_Z)$ extracted using the CT10 NLO PDF set. The fitted value for each $|y|$ bin; the corresponding uncertainty components due to PDF, scale, and nonperturbative corrections; and the total experimental uncertainty is shown. The last row of the table shows the results of combined fitting of all the $|y|$ bins simultaneously.

$ y $ bin	Fitted $\alpha_S(M_Z)$	PDF unc.	scale unc.	NP unc.	exp unc.	$\chi^2_{\min}/N_{\text{Bins}}$
0.0–0.5	0.1155	+0.0027 −0.0027	+0.0070 −0.0026	+0.0003 −0.0003	+0.0025 −0.0025	48.6/37
0.5–1.0	0.1156	+0.0025 −0.0026	+0.0069 −0.0026	+0.0003 −0.0003	+0.0026 −0.0025	28.4/37
1.0–1.5	0.1177	+0.0024 −0.0026	+0.0062 −0.0027	+0.0002 −0.0002	+0.0024 −0.0026	19.3/36
1.5–2.0	0.1163	+0.0025 −0.0029	+0.0040 −0.0019	+0.0002 −0.0002	+0.0023 −0.0027	65.6/32
2.0–2.5	0.1164	+0.0020 −0.0022	+0.0046 −0.0024	+0.0002 −0.0002	+0.0019 −0.0022	38.3/25
2.5–3.0	0.1158	+0.0029 −0.0030	+0.0049 −0.0025	+0.0006 −0.0006	+0.0036 −0.0038	14.3/18
Combined	0.1164	+0.0025 −0.0029	+0.0053 −0.0028	+0.0001 −0.0001	+0.0014 −0.0015	186.5/185

D0 [49, 50], H1 [56], and ZEUS [57] experiments is shown in Fig. 13. The present measurement is in very good agreement with results obtained by previous experiments. The present analysis constrains the $\alpha_S(Q)$ running for Q between 86 GeV and 1.5 TeV, which is the highest scale at which α_S has been measured, to date.

Table 5: The extracted $\alpha_S(M_Z)$ values, the corresponding $\alpha_S(Q)$ values at the Q scale for each p_T range, and $\chi^2_{\min}/N_{\text{Bins}}$ are shown. Uncertainties are given for both α_S values.

p_T range (GeV)	Q (GeV)	$\alpha_S(M_Z)$	$\alpha_S(Q)$	$\chi^2_{\min}/N_{\text{Bins}}$
74–133	86.86	0.1171 $^{+0.0060}_{-0.0039}$	0.1180 $^{+0.0061}_{-0.0040}$	26.04/24
133–220	156.52	0.1159 $^{+0.0061}_{-0.0037}$	0.1073 $^{+0.0052}_{-0.0032}$	19.47/24
220–300	247.10	0.1161 $^{+0.0062}_{-0.0036}$	0.1012 $^{+0.0047}_{-0.0027}$	12.39/18
300–395	333.27	0.1163 $^{+0.0064}_{-0.0039}$	0.0976 $^{+0.0045}_{-0.0027}$	19.48/18
395–507	434.72	0.1167 $^{+0.0061}_{-0.0036}$	0.0947 $^{+0.0039}_{-0.0024}$	17.12/18
507–686	563.77	0.1170 $^{+0.0064}_{-0.0039}$	0.0921 $^{+0.0038}_{-0.0024}$	23.25/21
686–905	755.97	0.1171 $^{+0.0070}_{-0.0040}$	0.0891 $^{+0.0039}_{-0.0023}$	24.76/20
905–1410	1011.02	0.1160 $^{+0.0070}_{-0.0050}$	0.0857 $^{+0.0037}_{-0.0027}$	24.68/28
1410–2500	1508.04	0.1162 $^{+0.0070}_{-0.0062}$	0.0822 $^{+0.0034}_{-0.0031}$	18.79/14

9 The QCD analysis of the inclusive jet measurements

The CMS inclusive jet measurements at $\sqrt{s} = 7$ TeV probe the gluon and valence-quark distributions in the kinematic range $x > 0.01$ [29]. In this paper, we use the inclusive jet cross section measurements at $\sqrt{s} = 8$ TeV for $p_T > 74$ GeV in a QCD analysis at NLO together with the combined measurements of neutral- and charged-current cross sections of deep inelastic electron (positron)-proton scattering at HERA [13]. The correlations of the experimental uncertainties for the jet measurements and DIS cross sections are taken into account. The DIS

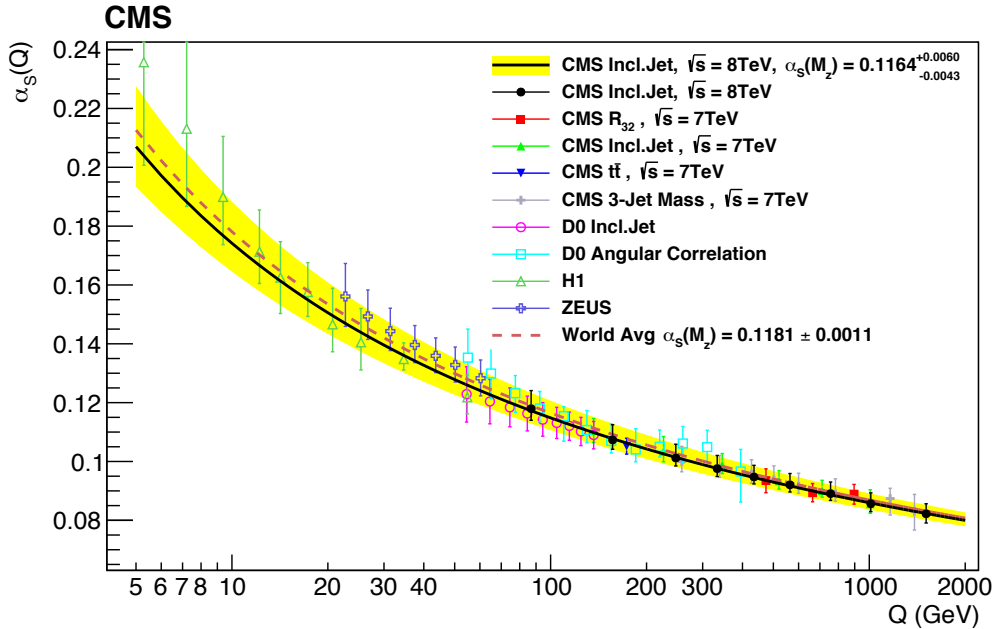


Figure 13: The running $\alpha_s(Q)$ as a function of the scale Q is shown, as obtained by using the CT10 NLO PDF set. The solid line and the uncertainty band are obtained by evolving the extracted $\alpha_s(M_Z)$ values by using the 2-loop 5-flavour renormalization group equations. The dashed line represents the evolution of the world average value. The black dots in the figure show the numbers obtained from the $\sqrt{s} = 8$ TeV inclusive jet measurement. Results from other CMS [53–55], D0 [49, 50], H1 [56], and ZEUS [57] measurements are superimposed.

measurements and the CMS jet cross section data are treated as uncorrelated. The theoretical predictions for the cross sections of jet production are calculated at NLO by using the NLO-JET++ program [32, 33] as implemented into the FASTNLO package [35]. The open-source QCD fit framework for PDF determination HERAFitter [58, 59], version 1.1.1, is used with the parton distributions evolved by using the DGLAP equations [60–65] at NLO, as implemented in the QCDNUM program [66].

The Thorne–Roberts general mass variable flavour number scheme at NLO [37, 67] is used for the treatment of the heavy-quark contributions with the heavy-quark masses $m_c = 1.47$ GeV and $m_b = 4.5$ GeV. The renormalization and factorization scales are set to Q , which denotes the four-momentum transfer in case of the DIS data and the jet p_T in case of the CMS jet cross sections.

The strong coupling constant is set to $\alpha_s(M_Z) = 0.118$, as in the HERAPDF2.0 analysis [13] and following the global PDF analyses, for example, in Ref. [39]. The Q^2 range of HERA data is restricted to $Q^2 \geq Q_{\min}^2 = 7.5$ GeV 2 .

The procedure for the determination of the PDFs follows the approach used in the previous QCD analysis [29] with the jet cross section measurements at $\sqrt{s} = 7$ TeV replaced by those at 8 TeV. At the initial scale of the QCD evolution $Q_0^2 = 1.9$ GeV 2 , the parton distributions are represented by:

Table 6: Composition of the uncertainty in $\alpha_S(M_Z)$ fit results in ranges of p_T . For each range, the corresponding statistical and experimental systematic uncertainties and the components of the theoretical uncertainty are shown. The numbers are obtained by using the CT10 NLO PDF set.

p_T range (GeV)	PDF unc.	scale unc.	NP unc.	stat unc.	syst unc.	exp unc.
74–133	+0.0007	+0.0054	+0.0004	+0.0016	+0.0020	+0.0026
	-0.0007	-0.0028	-0.0004	-0.0015	-0.0021	-0.0026
133–220	+0.0009	+0.0056	+0.0003	+0.0008	+0.0019	+0.0021
	-0.0009	-0.0029	-0.0003	-0.0008	-0.0019	-0.0021
220–300	+0.0013	+0.0058	+0.0003	+0.0003	+0.0018	+0.0018
	-0.0013	-0.0028	-0.0003	-0.0003	-0.0019	-0.0018
300–395	+0.0016	+0.0060	+0.0003	+0.0004	+0.0016	+0.0017
	-0.0017	-0.0030	-0.0003	-0.0004	-0.0016	-0.0017
395–507	+0.0018	+0.0056	+0.0002	+0.0007	+0.0014	+0.0016
	-0.0019	-0.0027	-0.0003	-0.0008	-0.0014	-0.0016
507–686	+0.0021	+0.0058	+0.0002	+0.0006	+0.0014	+0.0015
	-0.0022	-0.0029	-0.0003	-0.0007	-0.0013	-0.0015
686–905	+0.0024	+0.0062	+0.0002	+0.0014	+0.0015	+0.0021
	-0.0025	-0.0031	-0.0002	-0.0016	-0.0014	-0.0022
905–1410	+0.0026	+0.0058	+0.0001	+0.0021	+0.0017	+0.0027
	-0.0028	-0.0027	-0.0002	-0.0026	-0.0017	-0.0031
1410–2500	+0.0029	+0.0050	+0.0001	+0.0035	+0.0019	+0.0040
	-0.0032	-0.0033	-0.0001	-0.0037	-0.0020	-0.0042

$$xg(x) = A_g x^{B_g} (1-x)^{C_g} (1+E_g x^2) - A'_g x^{B'_g} (1-x)^{C'_g}, \quad (5)$$

$$xu_v(x) = A_{u_v} x^{B_{u_v}} (1-x)^{C_{u_v}} (1+D_{u_v} x + E_{u_v} x^2), \quad (6)$$

$$xd_v(x) = A_{d_v} x^{B_{d_v}} (1-x)^{C_{d_v}} (1+D_{d_v} x), \quad (7)$$

$$x\bar{U}(x) = A_{\bar{U}} x^{B_{\bar{U}}} (1-x)^{C_{\bar{U}}} (1+D_{\bar{U}} x), \quad (8)$$

$$x\bar{D}(x) = A_{\bar{D}} x^{B_{\bar{D}}} (1-x)^{C_{\bar{D}}} (1+D_{\bar{D}} x + E_{\bar{D}} x^2). \quad (9)$$

The normalization parameters A_{u_v} , A_{d_v} , A_g are determined by the QCD sum rules; the B parameter is responsible for small- x behavior of the PDFs; and the parameter C describes the shape of the distribution as $x \rightarrow 1$. A flexible form for the gluon distribution is adopted here, where the (fixed) choice of $C'_g = 25$ is motivated by the approach of the MSTW group [37, 67]. Additional constraints $B_{\bar{U}} = B_{\bar{D}}$ and $A_{\bar{U}} = A_{\bar{D}}(1-f_s)$ are imposed with f_s being the strangeness fraction, $f_s = \bar{s}/(\bar{d}+\bar{s})$, fixed to $f_s = 0.31 \pm 0.08$, as in Ref. [37], consistent with the determination of the strangeness fraction made by using the CMS measurements of W+charm production [68]. Additional D and E parameters allow probing the sensitivity of results on the specific selected functional form. The parameters in Eqs.(5)–(9) are selected by first fitting with all D and E parameters set to zero. The other parameters are then included in the fit one at a time. The improvement in χ^2 of the fits is monitored and the procedure is stopped when no further improvement is observed. This leads to an 18-parameter fit.

The PDF uncertainties are estimated in a way similar to the earlier CMS analyses [29, 68] according to the general approach of HERAPDF1.0 [40] in which experimental, model, and parameterization uncertainties are taken into account. The experimental uncertainties originate from the measurements included in the analysis and are determined by using the Hessian [69] method, applying a tolerance criterion of $\Delta\chi^2 = 1$. Alternatively, the Monte Carlo method [70, 71] to determine the PDF uncertainties is used.

Model uncertainties arise from variations in the values assumed for the charm and bottom

quark masses m_c and m_b , with $1.41 \leq m_c \leq 1.53 \text{ GeV}$ and $4.25 \leq m_b \leq 4.75 \text{ GeV}$, following Ref. [13], and the value of Q_{\min}^2 imposed on the HERA data, which is varied within the interval $5.0 \leq Q_{\min}^2 \leq 10.0 \text{ GeV}^2$. The strangeness fraction f_s is varied by its uncertainty.

The parameterization uncertainty is estimated by extending the functional form of all PDFs with additional parameters. The uncertainty is constructed as an envelope built from the maximal differences between the PDFs resulting from all the parameterization variations and the central fit at each x value.

The total PDF uncertainty is obtained by adding experimental, model, and parameterization uncertainties in quadrature. In the following, the quoted uncertainties correspond to 68% confidence level. The global and partial χ^2 values for each data set are listed in Table 7, where the χ^2 values illustrate a general agreement among all the data sets. The somewhat high χ^2/N_{dof} values for the combined DIS data are very similar to those observed in Ref. [13], where they are investigated in detail.

Table 7: Partial χ^2/N_{dp} per number of data points N_{dp} and the global χ^2 per degree of freedom, N_{dof} , as obtained in the QCD analysis of HERA DIS data and the CMS measurements of inclusive jet production at $\sqrt{s} = 8 \text{ TeV}$.

Data sets		Partial χ^2/N_{dp}
HERA I+II neutral current	$e^+ p, E_p = 920 \text{ GeV}$	376/332
HERA I+II neutral current	$e^+ p, E_p = 820 \text{ GeV}$	61/63
HERA I+II neutral current	$e^+ p, E_p = 575 \text{ GeV}$	197/234
HERA I+II neutral current	$e^+ p, E_p = 460 \text{ GeV}$	204/187
HERA I+II neutral current	$e^- p$	219/159
HERA I+II charged current	$e^+ p$	41/39
HERA I+II charged current	$e^- p$	50/42
CMS inclusive jets 8 TeV	$0 < y < 0.5$	53/36
	$0.5 < y < 1.0$	34/36
	$1.0 < y < 1.5$	35/35
	$1.5 < y < 2.0$	52/29
	$2.0 < y < 2.5$	49/24
	$2.5 < y < 3.0$	4.9/18
Correlated χ^2		94
Global χ^2/N_{dof}		1471/1216

Together with HERA DIS cross section data, the inclusive jet measurements provide important constraints on the gluon and valence-quark distributions in the kinematic range studied. These constraints are illustrated in Figs. 14 and 15, where the distributions of the gluon and valence quarks are shown at the scales of $Q^2 = 1.9$ and 10^5 GeV^2 , respectively. The results obtained using the Monte Carlo method to determine the PDF uncertainties are consistent with those obtained with the Hessian method. The uncertainties for the gluon distribution, as estimated by using the HERAPDF method for HERA-only and HERA+CMS jet analyses, are shown in Fig. 16. The parameterization uncertainty is significantly reduced once the CMS jet measurements are included.

The same QCD analysis has been performed using both the low- and high- p_T measurements of the jet cross sections at 8 TeV and including the systematic correlations of the two CMS data

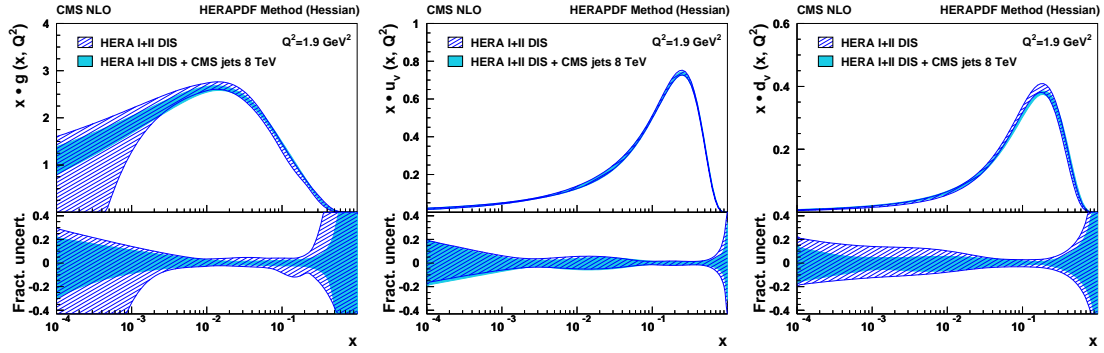


Figure 14: Gluon (left), u-valence quark (middle), and d-valence quark (right) distributions as functions of x at the starting scale $Q^2 = 1.9 \text{ GeV}^2$. The results of the fit to the HERA data and inclusive jet measurements at 8 TeV (shaded band), and to HERA data only (hatched band) are compared with their total uncertainties as determined by using the HERAPDF method. In the bottom panels the fractional uncertainties are shown.

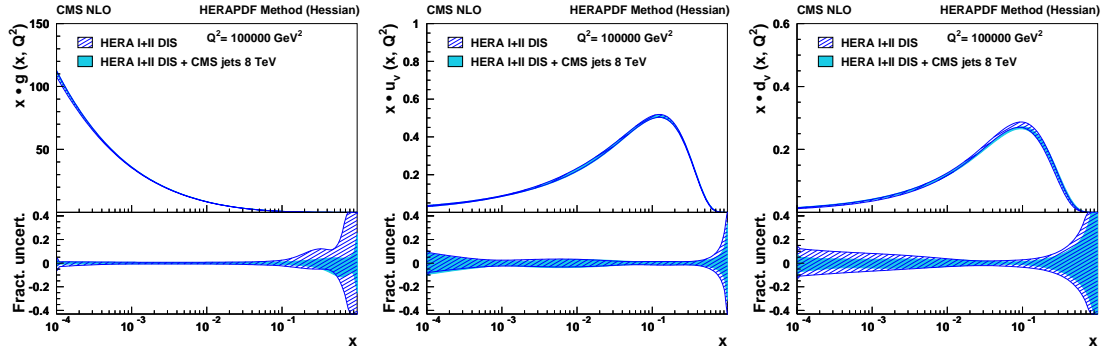


Figure 15: Same as Fig. 14, but for the scale of $Q^2 = 10^5 \text{ GeV}^2$.

sets. The PDFs obtained with the addition of the low- p_T jet cross sections are consistent with those from the high- p_T jet cross sections alone; the low- p_T jet cross sections do not, however, improve the PDF uncertainties significantly.

The gluon PDFs obtained from the 8 TeV jet cross sections are compared to those from the 7 TeV cross sections [29] in Fig. 17. The results are very similar.

The extraction of the PDFs from the jet cross sections depends on the value of α_S . Consequently, the PDF fits are repeated taking α_S to be a free parameter. In this way, the PDFs and the strong coupling constant are determined simultaneously, diminishing the correlation between the gluon PDF and α_S . The experimental, model, and parameterization uncertainties of $\alpha_S(M_Z)$ are obtained in a manner similar to the procedure for determining uncertainties of the PDFs. The uncertainty due to missing higher-order corrections in the theoretical predictions for jet production cross sections is estimated by varying the renormalization and factorization scales. The scales are varied independently by a factor of two with respect to the default choice of μ_R and μ_F equal to the p_T of the jet and the combined fit of PDFs and $\alpha_S(M_Z)$ is repeated for each variation of the scale choice in the following six combinations: $(\mu_R/p_T, \mu_F/p_T) = (0.5, 0.5), (0.5, 1), (1, 0.5), (1, 2), (2, 1)$, and $(2, 2)$. The scale for the HERA DIS data is not changed. The maximal observed upward and downward changes of $\alpha_S(M_Z)$ with respect to the default are then taken as the scale uncertainty. The strong coupling constant is $\alpha_S(M_Z) = 0.1185^{+0.0019}_{-0.0021} (\exp)^{+0.0002}_{-0.0015} (\text{model})^{+0.0000}_{-0.0004} (\text{param})^{+0.0022}_{-0.0018} (\text{scale})$. Within the uncertainties, this value is consistent with the one determined in Section 8 and is an important cross-

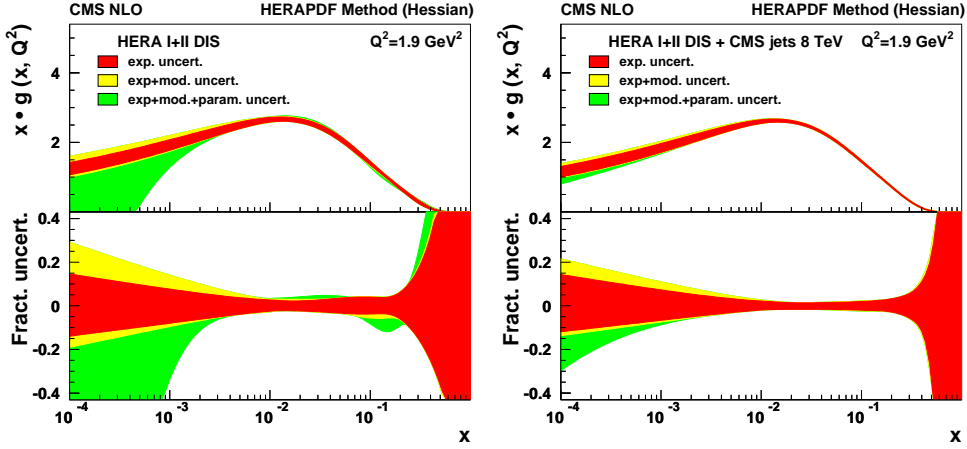


Figure 16: Gluon PDF distribution as a function of x at the starting scale $Q^2 = 1.9 \text{ GeV}^2$ as derived from HERA inclusive DIS (left) and in combination with CMS inclusive jet data (right). Different contributions to the PDF uncertainty are represented by bands of different shades. In the bottom panels the fractional uncertainties are shown.

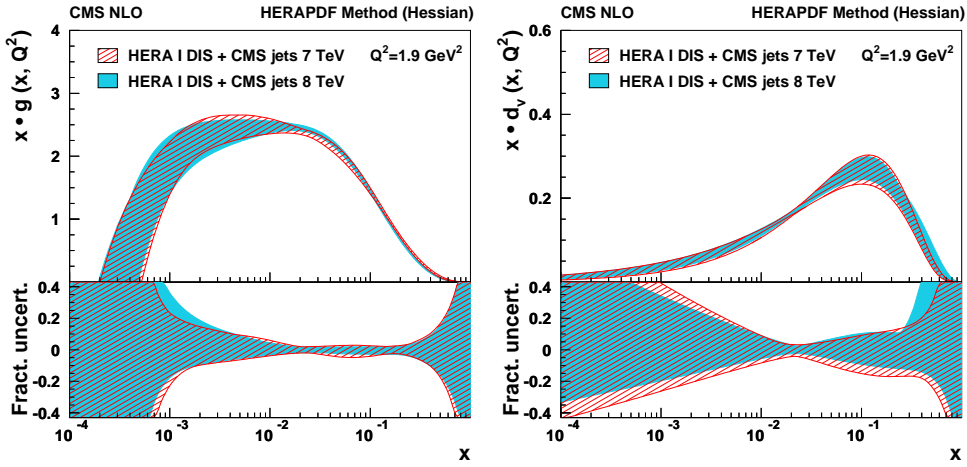


Figure 17: Gluon (left) and d-valence quark (right) distributions as functions of x at the starting scale $Q^2 = 1.9 \text{ GeV}^2$. The results of the 13-parameter fit [29] to the subset [40] of the combined HERA data and inclusive jet measurements at 7 TeV (hatched band), and, alternatively, 8 TeV (shaded band) are compared with their total uncertainties, as determined by using the HERAPDF method. In the bottom panels the fractional uncertainties are shown.

check of the $\alpha_S(M_Z)$ obtained by using the fixed PDF. The scale uncertainties in $\alpha_S(M_Z)$ obtained simultaneously with the PDFs are smaller due to consistent treatment of the scales in the PDFs and the theory prediction for the jet cross sections in the simultaneous fit. The evaluation of scale uncertainties is an open issue that is ignored in all global PDF fits to date. There is no recommended procedure for the determination of the scale uncertainties in combined fits of PDFs and $\alpha_S(M_Z)$.

10 Summary

A measurement of the double-differential inclusive jet cross section has been presented that uses data from proton-proton collisions at $\sqrt{s} = 8 \text{ TeV}$ collected with the CMS detector and

corresponding to an integrated luminosity of 19.7 fb^{-1} . The result is presented as a function of jet transverse momentum p_T and absolute rapidity $|y|$ and covers a large range in jet p_T from 74 GeV up to 2.5 TeV, in six rapidity bins up to $|y| = 3.0$. The region of low jet p_T , in particular the range from 21 to 74 GeV, has also been studied up to $|y| = 4.7$, using a dedicated low-pileup 5.6 pb^{-1} data sample. The ratios to the cross sections measured at 2.76 and 7 TeV have been also determined.

Detailed studies of experimental and theoretical sources of uncertainty have been carried out. The dominant sources of experimental systematic uncertainty are due to the jet energy scale, unfolding, and the integrated luminosity measurement. These lead to uncertainties of 5–45% in the differential cross section measurement. The theoretical predictions are most affected by PDF uncertainties, and their range is strongly dependent on the p_T and rapidity interval; at low p_T they are about 7%, but their size increases up to 40% in the most central intervals and exceeds 200% in the outermost regions. Many uncertainties cancel in the ratio with the corresponding results at 2.76 and 7 TeV, leading to uncertainties ranging from 5% to 25%, both for the measurement and for the theoretical predictions. Perturbative QCD, supplemented by a small nonperturbative and electroweak corrections, describes the data over a wide range of jet p_T and y .

The strong coupling constant is extracted from the high- p_T jet cross section measurements using the probed p_T range and six different rapidity bins. The best fitted value is $\alpha_S(M_Z) = 0.1164^{+0.0060}_{-0.0043}$ using the CT10 NLO PDF set. The running of the strong coupling constant as a function of the energy scale Q , $\alpha_S(Q)$, measured for nine different values of energy scale between 86 GeV and 1.5 TeV, is in good agreement with previous experiments and extends the measurement to the highest values of the energy scale.

This measurement of the double-differential jet cross section probes hadronic parton-parton interaction over a wide range of x and Q . The QCD analysis of these data together with HERA DIS measurements illustrates the potential of the high- p_T jet cross sections to provide important constraints on the gluon PDF in a new kinematic regime.

Acknowledgments

We congratulate our colleagues in the CERN accelerator departments for the excellent performance of the LHC and thank the technical and administrative staffs at CERN and at other CMS institutes for their contributions to the success of the CMS effort. In addition, we gratefully acknowledge the computing centres and personnel of the Worldwide LHC Computing Grid for delivering so effectively the computing infrastructure essential to our analyses. Finally, we acknowledge the enduring support for the construction and operation of the LHC and the CMS detector provided by the following funding agencies: the Austrian Federal Ministry of Science, Research and Economy and the Austrian Science Fund; the Belgian Fonds de la Recherche Scientifique, and Fonds voor Wetenschappelijk Onderzoek; the Brazilian Funding Agencies (CNPq, CAPES, FAPERJ, and FAPESP); the Bulgarian Ministry of Education and Science; CERN; the Chinese Academy of Sciences, Ministry of Science and Technology, and National Natural Science Foundation of China; the Colombian Funding Agency (COLCIENCIAS); the Croatian Ministry of Science, Education and Sport, and the Croatian Science Foundation; the Research Promotion Foundation, Cyprus; the Secretariat for Higher Education, Science, Technology and Innovation, Ecuador; the Ministry of Education and Research, Estonian Research Council via IUT23-4 and IUT23-6 and European Regional Development Fund, Estonia; the Academy of Finland, Finnish Ministry of Education and Culture, and Helsinki Institute of

Physics; the Institut National de Physique Nucléaire et de Physique des Particules / CNRS, and Commissariat à l'Énergie Atomique et aux Énergies Alternatives / CEA, France; the Bundesministerium für Bildung und Forschung, Deutsche Forschungsgemeinschaft, and Helmholtz-Gemeinschaft Deutscher Forschungszentren, Germany; the General Secretariat for Research and Technology, Greece; the National Scientific Research Foundation, and National Innovation Office, Hungary; the Department of Atomic Energy and the Department of Science and Technology, India; the Institute for Studies in Theoretical Physics and Mathematics, Iran; the Science Foundation, Ireland; the Istituto Nazionale di Fisica Nucleare, Italy; the Ministry of Science, ICT and Future Planning, and National Research Foundation (NRF), Republic of Korea; the Lithuanian Academy of Sciences; the Ministry of Education, and University of Malaya (Malaysia); the Mexican Funding Agencies (BUAP, CINVESTAV, CONACYT, LNS, SEP, and UASLP-FAI); the Ministry of Business, Innovation and Employment, New Zealand; the Pakistan Atomic Energy Commission; the Ministry of Science and Higher Education and the National Science Centre, Poland; the Fundação para a Ciência e a Tecnologia, Portugal; JINR, Dubna; the Ministry of Education and Science of the Russian Federation, the Federal Agency of Atomic Energy of the Russian Federation, Russian Academy of Sciences, and the Russian Foundation for Basic Research; the Ministry of Education, Science and Technological Development of Serbia; the Secretaría de Estado de Investigación, Desarrollo e Innovación and Programa Consolider-Ingenio 2010, Spain; the Swiss Funding Agencies (ETH Board, ETH Zurich, PSI, SNF, UniZH, Canton Zurich, and SER); the Ministry of Science and Technology, Taipei; the Thailand Center of Excellence in Physics, the Institute for the Promotion of Teaching Science and Technology of Thailand, Special Task Force for Activating Research and the National Science and Technology Development Agency of Thailand; the Scientific and Technical Research Council of Turkey, and Turkish Atomic Energy Authority; the National Academy of Sciences of Ukraine, and State Fund for Fundamental Researches, Ukraine; the Science and Technology Facilities Council, UK; the US Department of Energy, and the US National Science Foundation.

Individuals have received support from the Marie-Curie programme and the European Research Council and EPLANET (European Union); the Leventis Foundation; the A. P. Sloan Foundation; the Alexander von Humboldt Foundation; the Belgian Federal Science Policy Office; the Fonds pour la Formation à la Recherche dans l'Industrie et dans l'Agriculture (FRIA-Belgium); the Agentschap voor Innovatie door Wetenschap en Technologie (IWT-Belgium); the Ministry of Education, Youth and Sports (MEYS) of the Czech Republic; the Council of Science and Industrial Research, India; the HOMING PLUS programme of the Foundation for Polish Science, cofinanced from European Union, Regional Development Fund, the Mobility Plus programme of the Ministry of Science and Higher Education, the National Science Center (Poland), contracts Harmonia 2014/14/M/ST2/00428, Opus 2013/11/B/ST2/04202, 2014/13/B/ST2/02543 and 2014/15/B/ST2/03998, Sonata-bis 2012/07/E/ST2/01406; the Thalis and Aristeia programmes cofinanced by EU-ESF and the Greek NSRF; the National Priorities Research Program by Qatar National Research Fund; the Programa Clarín-COFUND del Principado de Asturias; the Rachadapisek Sompot Fund for Postdoctoral Fellowship, Chulalongkorn University and the Chulalongkorn Academic into Its 2nd Century Project Advancement Project (Thailand); and the Welch Foundation, contract C-1845.

References

- [1] ATLAS Collaboration, "Measurement of the inclusive jet cross section in pp collisions at $\sqrt{s} = 2.76$ TeV and comparison to the inclusive jet cross section at $\sqrt{s} = 7$ TeV using the ATLAS detector", *Eur. Phys. J. C* **73** (2013) 2509,
 doi:10.1140/epjc/s10052-013-2509-4, arXiv:1304.4739.

- [2] CMS Collaboration, “Measurement of the inclusive jet cross section in pp collisions at $\sqrt{s} = 2.76 \text{ TeV}$ ”, *Eur. Phys. J. C* **76** (2016), no. 5, 265,
doi:[10.1140/epjc/s10052-016-4083-z](https://doi.org/10.1140/epjc/s10052-016-4083-z), arXiv:[1512.06212](https://arxiv.org/abs/1512.06212).
- [3] ATLAS Collaboration, “Measurement of inclusive jet and dijet cross sections in proton-proton collisions at 7 TeV centre-of-mass energy with the ATLAS detector”, *Eur. Phys. J. C* **71** (2011) 1512, doi:[10.1140/epjc/s10052-010-1512-2](https://doi.org/10.1140/epjc/s10052-010-1512-2),
arXiv:[1009.5908](https://arxiv.org/abs/1009.5908).
- [4] CMS Collaboration, “Measurement of the inclusive jet cross section in pp collisions at 7 TeV”, *Phys. Rev. Lett.* **107** (2011) 132001, doi:[10.1103/PhysRevLett.107.132001](https://doi.org/10.1103/PhysRevLett.107.132001),
arXiv:[1106.0208](https://arxiv.org/abs/1106.0208).
- [5] ATLAS Collaboration, “Measurement of inclusive jet and dijet production in pp collisions at $\sqrt{s} = 7 \text{ TeV}$ using the ATLAS detector”, *Phys. Rev. D* **86** (2012) 014022,
doi:[10.1103/PhysRevD.86.014022](https://doi.org/10.1103/PhysRevD.86.014022), arXiv:[1112.6297](https://arxiv.org/abs/1112.6297).
- [6] CMS Collaboration, “Measurements of differential jet cross sections in proton-proton collisions at $\sqrt{s} = 7 \text{ TeV}$ with the CMS detector”, *Phys. Rev. D* **87** (2013) 112002,
doi:[10.1103/PhysRevD.87.112002](https://doi.org/10.1103/PhysRevD.87.112002), arXiv:[1212.6660](https://arxiv.org/abs/1212.6660).
- [7] UA2 Collaboration, “Observation of very large transverse momentum jets at the CERN $\bar{p}p$ collider”, *Phys. Lett. B* **118** (1982) 203, doi:[10.1016/0370-2693\(82\)90629-3](https://doi.org/10.1016/0370-2693(82)90629-3).
- [8] UA1 Collaboration, “Hadronic jet production at the CERN proton-antiproton collider”, *Phys. Lett. B* **132** (1983) 214, doi:[10.1016/0370-2693\(83\)90254-X](https://doi.org/10.1016/0370-2693(83)90254-X).
- [9] CDF Collaboration, “Measurement of the inclusive jet cross section using the k_T algorithm in $p\bar{p}$ collisions at $\sqrt{s} = 1.96 \text{ TeV}$ with the CDF II detector”, *Phys. Rev. D* **75** (2007) 092006, doi:[10.1103/PhysRevD.75.092006](https://doi.org/10.1103/PhysRevD.75.092006), arXiv:[hep-ex/0701051](https://arxiv.org/abs/hep-ex/0701051). [Erratum: doi:[10.1103/PhysRevD.75.119901](https://doi.org/10.1103/PhysRevD.75.119901)].
- [10] D0 Collaboration, “Measurement of the inclusive jet cross-section in $p\bar{p}$ collisions at $\sqrt{s} = 1.96 \text{ TeV}$ ”, *Phys. Rev. Lett.* **101** (2008) 062001,
doi:[10.1103/PhysRevLett.101.062001](https://doi.org/10.1103/PhysRevLett.101.062001), arXiv:[0802.2400](https://arxiv.org/abs/0802.2400).
- [11] CDF Collaboration, “Measurement of the inclusive jet cross section at the Fermilab Tevatron $p\bar{p}$ collider using a cone-based jet algorithm”, *Phys. Rev. D* **78** (2008) 052006,
doi:[10.1103/PhysRevD.78.052006](https://doi.org/10.1103/PhysRevD.78.052006), arXiv:[0807.2204](https://arxiv.org/abs/0807.2204). [Erratum: doi:[10.1103/PhysRevD.79.119902](https://doi.org/10.1103/PhysRevD.79.119902)].
- [12] M. L. Mangano and J. Rojo, “Cross section ratios between different CM energies at the LHC: opportunities for precision measurements and BSM sensitivity”, *JHEP* **08** (2012) 010, doi:[10.1007/JHEP08\(2012\)010](https://doi.org/10.1007/JHEP08(2012)010), arXiv:[1206.3557](https://arxiv.org/abs/1206.3557).
- [13] ZEUS and H1 Collaboration, “Combination of measurements of inclusive deep inelastic $e^\pm p$ scattering cross sections and QCD analysis of HERA data”, *Eur. Phys. J. C* **75** (2015) 580, doi:[10.1140/epjc/s10052-015-3710-4](https://doi.org/10.1140/epjc/s10052-015-3710-4), arXiv:[1506.06042](https://arxiv.org/abs/1506.06042).
- [14] CMS Collaboration, “The CMS experiment at the CERN LHC”, *JINST* **3** (2008) S08004,
doi:[10.1088/1748-0221/3/08/S08004](https://doi.org/10.1088/1748-0221/3/08/S08004).
- [15] CMS Collaboration, “Description and performance of track and primary-vertex reconstruction with the CMS tracker”, *JINST* **9** (2014) P10009,
doi:[10.1088/1748-0221/9/10/P10009](https://doi.org/10.1088/1748-0221/9/10/P10009), arXiv:[1405.6569](https://arxiv.org/abs/1405.6569).

- [16] CMS Collaboration, “Particle-flow event reconstruction in CMS and performance for jets, taus, and E_T^{miss} ”, CMS Physics Analysis Summary CMS-PAS-PFT-09-001, 2009.
- [17] CMS Collaboration, “Commissioning of the particle-flow event reconstruction with the first LHC collisions recorded in the CMS detector”, CMS Physics Analysis Summary CMS-PAS-PFT-10-001, 2010.
- [18] M. Cacciari, G. P. Salam, and G. Soyez, “The anti- k_t jet clustering algorithm”, *JHEP* **04** (2008) 063, doi:10.1088/1126-6708/2008/04/063, arXiv:0802.1189.
- [19] M. Cacciari, G. P. Salam, and G. Soyez, “FastJet user manual”, *Eur. Phys. J. C* **72** (2012) 1896, doi:10.1140/epjc/s10052-012-1896-2, arXiv:1111.6097.
- [20] GEANT4 Collaboration, “GEANT4—a simulation toolkit”, *Nucl. Inst. Meth. A* **506** (2003) 250, doi:10.1016/S0168-9002(03)01368-8.
- [21] CMS Collaboration, “Determination of jet energy calibration and transverse momentum resolution in CMS”, *JINST* **6** (2011) P11002, doi:10.1088/1748-0221/6/11/P11002, arXiv:1107.4277.
- [22] CMS Collaboration, “Jet energy scale and resolution in the CMS experiment in pp collisions at 8 TeV”, (2016). arXiv:1607.03663. Submitted to JINST.
- [23] T. Sjöstrand, S. Mrenna, and P. Skands, “PYTHIA 6.4 physics and manual”, *JHEP* **05** (2006) 026, doi:10.1088/1126-6708/2006/05/026, arXiv:hep-ph/0603175.
- [24] R. Field, “Early LHC underlying event data - findings and surprises”, in *Hadron collider physics. Proceedings, 22nd Conference, HCP 2010*. Toronto, Canada, 2010. arXiv:1010.3558.
- [25] J. Pumplin et al., “New generation of parton distributions with uncertainties from global QCD analysis”, *JHEP* **07** (2002) 012, doi:10.1088/1126-6708/2002/07/012, arXiv:hep-ph/0201195.
- [26] A. Buckley et al., “Systematic event generator tuning for the LHC”, *Eur. Phys. J. C* **65** (2010) 331, doi:10.1140/epjc/s10052-009-1196-7, arXiv:0907.2973.
- [27] G. D’Agostini, “A multidimensional unfolding method based on Bayes’ theorem”, *Nucl. Instrum. Meth. A* **362** (1995) 487, doi:10.1016/0168-9002(95)00274-X.
- [28] T. Adye, “Unfolding algorithms and tests using RooUnfold”, in *Proceedings of the PHYSTAT 2011 Workshop*, H. B. Prosper and L. Lyons, eds. CERN, Geneva, Switzerland, 2011. arXiv:1105.1160. doi:10.5170/CERN-2011-006.
- [29] CMS Collaboration, “Constraints on parton distribution functions and extraction of the strong coupling constant from the inclusive jet cross section in pp collisions at $\sqrt{s} = 7 \text{ TeV}$ ”, *Eur. Phys. J. C* **75** (2015) 288, doi:10.1140/epjc/s10052-015-3499-1, arXiv:1410.6765.
- [30] CMS Collaboration, “CMS luminosity based on pixel cluster counting — Summer 2013 update”, CMS Physics Analysis Summary CMS-PAS-LUM-13-001, CERN, Geneva, 2013.
- [31] CMS Collaboration, “CMS luminosity based on pixel cluster counting — Summer 2012 update”, CMS Physics Analysis Summary CMS-PAS-LUM-12-001, CERN, Geneva, 2012.

- [32] Z. Nagy, "Three-jet cross sections in hadron-hadron collisions at next-to-leading order", *Phys. Rev. Lett.* **88** (2002) 122003, doi:10.1103/PhysRevLett.88.122003, arXiv:hep-ph/0110315.
- [33] Z. Nagy, "Next-to-leading order calculation of three jet observables in hadron-hadron collision", *Phys. Rev. D* **68** (2003) 094002, doi:10.1103/PhysRevD.68.094002, arXiv:hep-ph/0307268.
- [34] S. Dittmaier, A. Huss, and C. Speckner, "Weak radiative corrections to dijet production at hadron colliders", *JHEP* **11** (2012) 095, doi:10.1007/JHEP11(2012)095, arXiv:1210.0438.
- [35] D. Britzger, K. Rabbertz, F. Stober, and M. Wobisch, "New features in version 2 of the fastNLO project", (2012). arXiv:1208.3641.
- [36] H.-L. Lai et al., "New parton distributions for collider physics", *Phys. Rev. D* **82** (2010) 074024, doi:10.1103/PhysRevD.82.074024, arXiv:1007.2241.
- [37] A. D. Martin, W. J. Stirling, R. S. Thorne, and G. Watt, "Parton distributions for the LHC", *Eur. Phys. J. C* **63** (2009) 189, doi:10.1140/epjc/s10052-009-1072-5, arXiv:0901.0002.
- [38] R. D. Ball et al., "A first unbiased global NLO determination of parton distributions and their uncertainties", *Nucl. Phys. B* **838** (2010) 136, doi:10.1016/j.nuclphysb.2010.05.008, arXiv:1002.4407.
- [39] R. D. Ball et al., "Parton distributions for the LHC Run II", *JHEP* **04** (2015) 040, doi:10.1007/JHEP04(2015)040, arXiv:1410.8849.
- [40] H1 and ZEUS Collaboration, "Combined measurement and QCD analysis of the inclusive $e^\pm p$ scattering cross sections at HERA", *JHEP* **01** (2010) 109, doi:10.1007/JHEP01(2010)109, arXiv:0911.0884.
- [41] S. Alekhin, J. Blümlein, and S. Moch, "Parton distribution functions and benchmark cross sections at NNLO", *Phys. Rev. D* **86** (2012) 054009, doi:10.1103/PhysRevD.86.054009, arXiv:1202.2281.
- [42] M. Bähr et al., "Herwig++ physics and manual", *Eur. Phys. J. C* **58** (2008) 639, doi:10.1140/epjc/s10052-008-0798-9, arXiv:0803.0883.
- [43] M. H. Seymour and A. Siódak, "Constraining MPI models using σ_{eff} and recent Tevatron and LHC underlying event data", *JHEP* **10** (2013) 113, doi:10.1007/JHEP10(2013)113, arXiv:1307.5015.
- [44] P. Nason, "A new method for combining NLO QCD with shower Monte Carlo algorithms", *JHEP* **11** (2004) 040, doi:10.1088/1126-6708/2004/11/040, arXiv:hep-ph/0409146.
- [45] S. Frixione, P. Nason, and C. Oleari, "Matching NLO QCD computations with parton shower simulations: the POWHEG method", *JHEP* **11** (2007) 070, doi:10.1088/1126-6708/2007/11/070, arXiv:0709.2092.
- [46] S. Alioli, P. Nason, C. Oleari, and E. Re, "A general framework for implementing NLO calculations in shower Monte Carlo programs: the POWHEG BOX", *JHEP* **06** (2010) 043, doi:10.1007/JHEP06(2010)043, arXiv:1002.2581.

- [47] S. Alioli et al., “Jet pair production in POWHEG”, *JHEP* **04** (2011) 081, doi:10.1007/JHEP04(2011)081, arXiv:1012.3380.
- [48] P. Z. Skands, “Tuning Monte Carlo generators: the Perugia tunes”, *Phys. Rev. D* **82** (2010) 074018, doi:10.1103/PhysRevD.82.074018, arXiv:1005.3457.
- [49] D0 Collaboration, “Determination of the strong coupling constant from the inclusive jet cross section in $p\bar{p}$ collisions at $\sqrt{s} = 1.96$ TeV”, *Phys. Rev. D* **80** (2009) 111107, doi:10.1103/PhysRevD.80.111107, arXiv:0911.2710.
- [50] D0 Collaboration, “Measurement of angular correlations of jets at $\sqrt{s} = 1.96$ TeV and determination of the strong coupling at high momentum transfers”, *Phys. Lett. B* **718** (2012) 56, doi:10.1016/j.physletb.2012.10.003, arXiv:1207.4957.
- [51] CDF Collaboration, “Measurement of the strong coupling constant from inclusive jet production at the Tevatron $\bar{p}p$ collider”, *Phys. Rev. Lett.* **88** (2002) 042001, doi:10.1103/PhysRevLett.88.042001, arXiv:hep-ex/0108034.
- [52] Particle Data Group Collaboration, “Review of Particle Physics”, *Chin. Phys. C* **40** (2016), no. 10, 100001, doi:10.1088/1674-1137/40/10/100001.
- [53] CMS Collaboration, “Measurement of the ratio of the inclusive 3-jet cross section to the inclusive 2-jet cross section in pp collisions at $\sqrt{s} = 7$ TeV and first determination of the strong coupling constant in the TeV range”, *Eur. Phys. J. C* **73** (2013) 2604, doi:10.1140/epjc/s10052-013-2604-6, arXiv:1304.7498.
- [54] CMS Collaboration, “Determination of the top-quark pole mass and strong coupling constant from the $t\bar{t}$ production cross section in pp collisions at $\sqrt{s} = 7$ TeV”, *Phys. Lett. B* **728** (2014) 496, doi:10.1016/j.physletb.2013.12.009, arXiv:1307.1907.
- [55] CMS Collaboration, “Measurement of the inclusive 3-jet production differential cross section in proton-proton collisions at 7 TeV and determination of the strong coupling constant in the TeV range”, *Eur. Phys. J. C* **75** (2015) 186, doi:10.1140/epjc/s10052-015-3376-y, arXiv:1412.1633.
- [56] H1 Collaboration, “Measurement of Jet Productio Cross Sections in Deep-inelastic ep Scattering at HERA”, (2016). arXiv:1611.03421.
- [57] ZEUS Collaboration, “Inclusive-jet photoproduction at HERA and determination of α_s ”, *Nucl. Phys. B* **864** (2012) 1, doi:10.1016/j.nuclphysb.2012.06.006, arXiv:1205.6153.
- [58] S. Alekhin et al., “HERAFitter, Open source QCD fit project”, *Eur. Phys. J. C* **75** (2015) 304, doi:10.1140/epjc/s10052-015-3480-z, arXiv:1410.4412.
- [59] HERAFitter Collaboration, <http://www.herafitter.org>.
- [60] V. N. Gribov and L. N. Lipatov, “Deep inelastic ep scattering in perturbation theory”, *Sov. J. Nucl. Phys.* **15** (1972) 438.
- [61] G. Altarelli and G. Parisi, “Asymptotic freedom in parton language”, *Nucl. Phys. B* **126** (1977) 298, doi:10.1016/0550-3213(77)90384-4.
- [62] G. Curci, W. Furmanski, and R. Petronzio, “Evolution of parton densities beyond leading order: The non-singlet case”, *Nucl. Phys. B* **175** (1980) 27, doi:10.1016/0550-3213(80)90003-6.

- [63] W. Furmanski and R. Petronzio, “Singlet parton densities beyond leading order”, *Phys. Lett. B* **97** (1980) 437, doi:10.1016/0370-2693(80)90636-X.
- [64] S. Moch, J. A. M. Vermaasen, and A. Vogt, “The three-loop splitting functions in QCD: the non-singlet case”, *Nucl. Phys. B* **688** (2004) 101, doi:10.1016/j.nuclphysb.2004.03.030, arXiv:hep-ph/0403192.
- [65] A. Vogt, S. Moch, and J. A. M. Vermaasen, “The three-loop splitting functions in QCD: the singlet case”, *Nucl. Phys. B* **691** (2004) 129, doi:10.1016/j.nuclphysb.2004.04.024, arXiv:hep-ph/0404111.
- [66] M. Botje, “QCDNUM: Fast QCD evolution and convolution”, *Comput. Phys. Commun.* **182** (2011) 490, doi:10.1016/j.cpc.2010.10.020, arXiv:1005.1481.
- [67] R. S. Thorne, “Variable-flavor number scheme for NNLO”, *Phys. Rev. D* **73** (2006) 054019, doi:10.1103/PhysRevD.73.054019, arXiv:hep-ph/0601245.
- [68] CMS Collaboration, “Measurement of the muon charge asymmetry in inclusive $\text{pp} \rightarrow W + X$ production at $\sqrt{s} = 7 \text{ TeV}$ and an improved determination of light parton distribution functions”, *Phys. Rev. D* **90** (2014) 032004, doi:10.1103/PhysRevD.90.032004, arXiv:1312.6283.
- [69] J. Pumplin et al., “Uncertainties of predictions from parton distribution functions. II. The Hessian method”, *Phys. Rev. D* **65** (2001) 014013, doi:10.1103/PhysRevD.65.014013, arXiv:hep-ph/0101032.
- [70] W. T. Giele and S. Keller, “Implications of hadron collider observables on parton distribution function uncertainties”, *Phys. Rev. D* **58** (1998) 094023, doi:10.1103/PhysRevD.58.094023, arXiv:hep-ph/9803393.
- [71] W. T. Giele, S. A. Keller, and D. A. Kosower, “Parton distribution function uncertainties”, (2001). arXiv:hep-ph/0104052.

A The CMS Collaboration

Yerevan Physics Institute, Yerevan, Armenia
V. Khachatryan, A.M. Sirunyan, A. Tumasyan

Institut für Hochenergiephysik der OeAW, Wien, Austria

W. Adam, E. Asilar, T. Bergauer, J. Brandstetter, E. Brondolin, M. Dragicevic, J. Erö, M. Flechl, M. Friedl, R. Frühwirth¹, V.M. Ghete, C. Hartl, N. Hörmann, J. Hrubec, M. Jeitler¹, A. König, I. Krätschmer, D. Liko, T. Matsushita, I. Mikulec, D. Rabady, N. Rad, B. Rahbaran, H. Rohringer, J. Schieck¹, J. Strauss, W. Treberer-Treberspurg, W. Waltenberger, C.-E. Wulz¹

National Centre for Particle and High Energy Physics, Minsk, Belarus
V. Mossolov, N. Shumeiko, J. Suarez Gonzalez

Universiteit Antwerpen, Antwerpen, Belgium

S. Alderweireldt, E.A. De Wolf, X. Janssen, J. Lauwers, M. Van De Klundert, H. Van Haevermaet, P. Van Mechelen, N. Van Remortel, A. Van Spilbeeck

Vrije Universiteit Brussel, Brussel, Belgium

S. Abu Zeid, F. Blekman, J. D'Hondt, N. Daci, I. De Bruyn, K. Deroover, N. Heracleous, S. Lowette, S. Moortgat, L. Moreels, A. Olbrechts, Q. Python, S. Tavernier, W. Van Doninck, P. Van Mulders, I. Van Parijs

Université Libre de Bruxelles, Bruxelles, Belgium

H. Brun, C. Caillol, B. Clerbaux, G. De Lentdecker, H. Delannoy, G. Fasanella, L. Favart, R. Goldouzian, A. Grebenyuk, G. Karapostoli, T. Lenzi, A. Léonard, J. Luetic, T. Maerschalk, A. Marinov, A. Randle-conde, T. Seva, C. Vander Velde, P. Vanlaer, R. Yonamine, F. Zenoni, F. Zhang²

Ghent University, Ghent, Belgium

A. Cimmino, T. Cornelis, D. Dobur, A. Fagot, G. Garcia, M. Gul, D. Poyraz, S. Salva, R. Schöfbeck, M. Tytgat, W. Van Driessche, E. Yazgan, N. Zaganidis

Université Catholique de Louvain, Louvain-la-Neuve, Belgium

C. Beluffi³, O. Bondu, S. Brochet, G. Bruno, A. Caudron, L. Ceard, S. De Visscher, C. Delaere, M. Delcourt, L. Forthomme, B. Francois, A. Giannanco, A. Jafari, P. Jez, M. Komm, V. Lemaitre, A. Magitteri, A. Mertens, M. Musich, C. Nuttens, K. Piotrzkowski, L. Quertenmont, M. Selvaggi, M. Vidal Marono, S. Wertz

Université de Mons, Mons, Belgium

N. Belyi

Centro Brasileiro de Pesquisas Fisicas, Rio de Janeiro, Brazil

W.L. Aldá Júnior, F.L. Alves, G.A. Alves, L. Brito, C. Hensel, A. Moraes, M.E. Pol, P. Rebello Teles

Universidade do Estado do Rio de Janeiro, Rio de Janeiro, Brazil

E. Belchior Batista Das Chagas, W. Carvalho, J. Chinellato⁴, A. Custódio, E.M. Da Costa, G.G. Da Silveira, D. De Jesus Damiao, C. De Oliveira Martins, S. Fonseca De Souza, L.M. Huertas Guativa, H. Malbouisson, D. Matos Figueiredo, C. Mora Herrera, L. Mundim, H. Nogima, W.L. Prado Da Silva, A. Santoro, A. Sznajder, E.J. Tonelli Manganote⁴, A. Vilela Pereira

Universidade Estadual Paulista ^a, Universidade Federal do ABC ^b, São Paulo, Brazil

S. Ahuja^a, C.A. Bernardes^b, S. Dogra^a, T.R. Fernandez Perez Tomei^a, E.M. Gregores^b,

P.G. Mercadante^b, C.S. Moon^{a,5}, S.F. Novaes^a, Sandra S. Padula^a, D. Romero Abad^b, J.C. Ruiz Vargas

Institute for Nuclear Research and Nuclear Energy, Sofia, Bulgaria

A. Aleksandrov, R. Hadjiiska, P. Iaydjiev, M. Rodozov, S. Stoykova, G. Sultanov, M. Vutova

University of Sofia, Sofia, Bulgaria

A. Dimitrov, I. Glushkov, L. Litov, B. Pavlov, P. Petkov

Beihang University, Beijing, China

W. Fang⁶

Institute of High Energy Physics, Beijing, China

M. Ahmad, J.G. Bian, G.M. Chen, H.S. Chen, M. Chen, Y. Chen⁷, T. Cheng, C.H. Jiang, D. Leggat, Z. Liu, F. Romeo, S.M. Shaheen, A. Spiezia, J. Tao, C. Wang, Z. Wang, H. Zhang, J. Zhao

State Key Laboratory of Nuclear Physics and Technology, Peking University, Beijing, China

C. Asawatangtrakuldee, Y. Ban, Q. Li, S. Liu, Y. Mao, S.J. Qian, D. Wang, Z. Xu

Universidad de Los Andes, Bogota, Colombia

C. Avila, A. Cabrera, L.F. Chaparro Sierra, C. Florez, J.P. Gomez, C.F. González Hernández, J.D. Ruiz Alvarez, J.C. Sanabria

University of Split, Faculty of Electrical Engineering, Mechanical Engineering and Naval Architecture, Split, Croatia

N. Godinovic, D. Lelas, I. Puljak, P.M. Ribeiro Cipriano

University of Split, Faculty of Science, Split, Croatia

Z. Antunovic, M. Kovac

Institute Rudjer Boskovic, Zagreb, Croatia

V. Brigljevic, D. Ferencek, K. Kadija, S. Micanovic, L. Sudic

University of Cyprus, Nicosia, Cyprus

A. Attikis, G. Mavromanolakis, J. Mousa, C. Nicolaou, F. Ptochos, P.A. Razis, H. Rykaczewski

Charles University, Prague, Czech Republic

M. Finger⁸, M. Finger Jr.⁸

Universidad San Francisco de Quito, Quito, Ecuador

E. Carrera Jarrin

Academy of Scientific Research and Technology of the Arab Republic of Egypt, Egyptian Network of High Energy Physics, Cairo, Egypt

Y. Assran^{9,10}, T. Elkafrawy¹¹, A. Ellithi Kamel¹², A. Mahrous¹³

National Institute of Chemical Physics and Biophysics, Tallinn, Estonia

B. Calpas, M. Kadastik, M. Murumaa, L. Perrini, M. Raidal, A. Tiko, C. Veelken

Department of Physics, University of Helsinki, Helsinki, Finland

P. Eerola, J. Pekkanen, M. Voutilainen

Helsinki Institute of Physics, Helsinki, Finland

J. Hätkönen, V. Karimäki, R. Kinnunen, T. Lampén, K. Lassila-Perini, S. Lehti, T. Lindén, P. Luukka, T. Peltola, J. Tuominiemi, E. Tuovinen, L. Wendland

Lappeenranta University of Technology, Lappeenranta, Finland

J. Talvitie, T. Tuuva

IRFU, CEA, Université Paris-Saclay, Gif-sur-Yvette, France

M. Besancon, F. Couderc, M. Dejardin, D. Denegri, B. Fabbro, J.L. Faure, C. Favaro, F. Ferri, S. Ganjour, S. Ghosh, A. Givernaud, P. Gras, G. Hamel de Monchenault, P. Jarry, I. Kucher, E. Locci, M. Machet, J. Rander, A. Rosowsky, M. Titov, A. Zghiche

Laboratoire Leprince-Ringuet, Ecole Polytechnique, IN2P3-CNRS, Palaiseau, France

A. Abdulsalam, I. Antropov, S. Baffioni, F. Beaudette, P. Busson, L. Cadamuro, E. Chapon, C. Charlot, O. Davignon, R. Granier de Cassagnac, M. Jo, S. Lisniak, P. Miné, I.N. Naranjo, M. Nguyen, C. Ochando, G. Ortona, P. Paganini, P. Pigard, S. Regnard, R. Salerno, Y. Sirois, T. Strebler, Y. Yilmaz, A. Zabi

Institut Pluridisciplinaire Hubert Curien, Université de Strasbourg, Université de Haute Alsace Mulhouse, CNRS/IN2P3, Strasbourg, FranceJ.-L. Agram¹⁴, J. Andrea, A. Aubin, D. Bloch, J.-M. Brom, M. Buttignol, E.C. Chabert, N. Chanon, C. Collard, E. Conte¹⁴, X. Coubez, J.-C. Fontaine¹⁴, D. Gelé, U. Goerlach, A.-C. Le Bihan, J.A. Merlin¹⁵, K. Skovpen, P. Van Hove**Centre de Calcul de l’Institut National de Physique Nucléaire et de Physique des Particules, CNRS/IN2P3, Villeurbanne, France**

S. Gadrat

Université de Lyon, Université Claude Bernard Lyon 1, CNRS-IN2P3, Institut de Physique Nucléaire de Lyon, Villeurbanne, FranceS. Beauceron, C. Bernet, G. Boudoul, E. Bouvier, C.A. Carrillo Montoya, R. Chierici, D. Contardo, B. Courbon, P. Depasse, H. El Mamouni, J. Fan, J. Fay, S. Gascon, M. Gouzevitch, G. Grenier, B. Ille, F. Lagarde, I.B. Laktineh, M. Lethuillier, L. Mirabito, A.L. Pequegnot, S. Perries, A. Popov¹⁶, D. Sabes, V. Sordini, M. Vander Donckt, P. Verdier, S. Viret**Georgian Technical University, Tbilisi, Georgia**A. Khvedelidze⁸**Tbilisi State University, Tbilisi, Georgia**

D. Lomidze

RWTH Aachen University, I. Physikalisches Institut, Aachen, GermanyC. Autermann, S. Beranek, L. Feld, A. Heister, M.K. Kiesel, K. Klein, M. Lipinski, A. Ostapchuk, M. Preuten, F. Raupach, S. Schael, C. Schomakers, J.F. Schulte, J. Schulz, T. Verlage, H. Weber, V. Zhukov¹⁶**RWTH Aachen University, III. Physikalisches Institut A, Aachen, Germany**

M. Brodski, E. Dietz-Laursonn, D. Duchardt, M. Endres, M. Erdmann, S. Erdweg, T. Esch, R. Fischer, A. Güth, T. Hebbeker, C. Heidemann, K. Hoepfner, S. Knutzen, M. Merschmeyer, A. Meyer, P. Millet, S. Mukherjee, M. Olszewski, K. Padeken, P. Papacz, T. Pook, M. Radziej, H. Reithler, M. Rieger, F. Scheuch, L. Sonnenschein, D. Teyssier, S. Thüer

RWTH Aachen University, III. Physikalisches Institut B, Aachen, GermanyV. Cherepanov, Y. Erdogan, G. Flügge, F. Hoehle, B. Kargoll, T. Kress, A. Künsken, J. Lingemann, A. Nehrkorn, A. Nowack, I.M. Nugent, C. Pistone, O. Pooth, A. Stahl¹⁵**Deutsches Elektronen-Synchrotron, Hamburg, Germany**M. Aldaya Martin, I. Asin, K. Beernaert, O. Behnke, U. Behrens, A.A. Bin Anuar, K. Borras¹⁷, A. Campbell, P. Connor, C. Contreras-Campana, F. Costanza, C. Diez Pardos, G. Dolinska,

G. Eckerlin, D. Eckstein, E. Eren, E. Gallo¹⁸, J. Garay Garcia, A. Geiser, A. Gizhko, J.M. Grados Luyando, P. Gunnellini, A. Harb, J. Hauk, M. Hempel¹⁹, H. Jung, A. Kalogeropoulos, O. Karacheban¹⁹, M. Kasemann, J. Keaveney, J. Kieseler, C. Kleinwort, I. Korol, O. Kuprash, W. Lange, A. Lelek, J. Leonard, K. Lipka, A. Lobanov, W. Lohmann¹⁹, R. Mankel, I.-A. Melzer-Pellmann, A.B. Meyer, G. Mittag, J. Mnich, A. Mussgiller, E. Ntomari, D. Pitzl, R. Placakyte, A. Raspereza, B. Roland, M.Ö. Sahin, P. Saxena, T. Schoerner-Sadenius, C. Seitz, S. Spannagel, N. Stefaniuk, K.D. Trippkewitz, G.P. Van Onsem, R. Walsh, C. Wissing

University of Hamburg, Hamburg, Germany

V. Blobel, M. Centis Vignali, A.R. Draeger, T. Dreyer, E. Garutti, K. Goebel, D. Gonzalez, J. Haller, M. Hoffmann, A. Junkes, R. Klanner, R. Kogler, N. Kovalchuk, T. Lapsien, T. Lenz, I. Marchesini, D. Marconi, M. Meyer, M. Niedziela, D. Nowatschin, J. Ott, F. Pantaleo¹⁵, T. Peiffer, A. Perieanu, J. Poehlsen, C. Sander, C. Scharf, P. Schleper, A. Schmidt, S. Schumann, J. Schwandt, H. Stadie, G. Steinbrück, F.M. Stober, M. Stöver, H. Tholen, D. Troendle, E. Usai, L. Vanelderen, A. Vanhoefer, B. Vormwald

Institut für Experimentelle Kernphysik, Karlsruhe, Germany

C. Barth, C. Baus, J. Berger, E. Butz, T. Chwalek, F. Colombo, W. De Boer, A. Dierlamm, S. Fink, R. Friese, M. Giffels, A. Gilbert, D. Haitz, F. Hartmann¹⁵, S.M. Heindl, U. Husemann, I. Katkov¹⁶, A. Kornmayer¹⁵, P. Lobelle Pardo, B. Maier, H. Mildner, M.U. Mozer, T. Müller, Th. Müller, M. Plagge, G. Quast, K. Rabbertz, S. Röcker, F. Roscher, M. Schröder, G. Sieber, H.J. Simonis, R. Ulrich, J. Wagner-Kuhr, S. Wayand, M. Weber, T. Weiler, S. Williamson, C. Wöhrmann, R. Wolf

Institute of Nuclear and Particle Physics (INPP), NCSR Demokritos, Aghia Paraskevi, Greece

G. Anagnostou, G. Daskalakis, T. Geralis, V.A. Giakoumopoulou, A. Kyriakis, D. Loukas, I. Topsis-Giotis

National and Kapodistrian University of Athens, Athens, Greece

A. Agapitos, S. Kesisoglou, A. Panagiotou, N. Saoulidou, E. Tziaferi

University of Ioánnina, Ioánnina, Greece

I. Evangelou, G. Flouris, C. Foudas, P. Kokkas, N. Loukas, N. Manthos, I. Papadopoulos, E. Paradas

MTA-ELTE Lendület CMS Particle and Nuclear Physics Group, Eötvös Loránd University, Budapest, Hungary

N. Filipovic

Wigner Research Centre for Physics, Budapest, Hungary

G. Bencze, C. Hajdu, P. Hidas, D. Horvath²⁰, F. Sikler, V. Veszpremi, G. Vesztergombi²¹, A.J. Zsigmond

Institute of Nuclear Research ATOMKI, Debrecen, Hungary

N. Beni, S. Czellar, J. Karancsi²², J. Molnar, Z. Szillasi

University of Debrecen, Debrecen, Hungary

M. Bartók²¹, A. Makovec, P. Raics, Z.L. Trocsanyi, B. Ujvari

National Institute of Science Education and Research, Bhubaneswar, India

S. Bahinipati, S. Choudhury²³, P. Mal, K. Mandal, A. Nayak²⁴, D.K. Sahoo, N. Sahoo, S.K. Swain

Panjab University, Chandigarh, India

S. Bansal, S.B. Beri, V. Bhatnagar, R. Chawla, R. Gupta, U.Bhawandeep, A.K. Kalsi, A. Kaur, M. Kaur, R. Kumar, A. Mehta, M. Mittal, J.B. Singh, G. Walia

University of Delhi, Delhi, India

Ashok Kumar, A. Bhardwaj, B.C. Choudhary, R.B. Garg, S. Keshri, A. Kumar, S. Malhotra, M. Naimuddin, N. Nishu, K. Ranjan, R. Sharma, V. Sharma

Saha Institute of Nuclear Physics, Kolkata, India

R. Bhattacharya, S. Bhattacharya, K. Chatterjee, S. Dey, S. Dutt, S. Dutta, S. Ghosh, N. Majumdar, A. Modak, K. Mondal, S. Mukhopadhyay, S. Nandan, A. Purohit, A. Roy, D. Roy, S. Roy Chowdhury, S. Sarkar, M. Sharan, S. Thakur

Indian Institute of Technology Madras, Madras, India

P.K. Behera

Bhabha Atomic Research Centre, Mumbai, India

R. Chudasama, D. Dutta, V. Jha, V. Kumar, A.K. Mohanty¹⁵, P.K. Netrakanti, L.M. Pant, P. Shukla, A. Topkar

Tata Institute of Fundamental Research-A, Mumbai, India

T. Aziz, S. Dugad, G. Kole, B. Mahakud, S. Mitra, G.B. Mohanty, N. Sur, B. Sutar

Tata Institute of Fundamental Research-B, Mumbai, India

S. Banerjee, S. Bhowmik²⁵, R.K. Dewanjee, S. Ganguly, M. Guchait, Sa. Jain, S. Kumar, M. Maity²⁵, G. Majumder, K. Mazumdar, B. Parida, T. Sarkar²⁵, N. Wickramage²⁶

Indian Institute of Science Education and Research (IISER), Pune, India

S. Chauhan, S. Dube, A. Kapoor, K. Kothekar, A. Rane, S. Sharma

Institute for Research in Fundamental Sciences (IPM), Tehran, Iran

H. Bakhshiansohi, H. Behnamian, S. Chenarani²⁷, E. Eskandari Tadavani, S.M. Etesami²⁷, A. Fahim²⁸, M. Khakzad, M. Mohammadi Najafabadi, M. Naseri, S. Paktnat Mehdiabadi, F. Rezaei Hosseinabadi, B. Safarzadeh²⁹, M. Zeinali

University College Dublin, Dublin, Ireland

M. Felcini, M. Grunewald

INFN Sezione di Bari ^a, Università di Bari ^b, Politecnico di Bari ^c, Bari, Italy

M. Abbrescia^{a,b}, C. Calabria^{a,b}, C. Caputo^{a,b}, A. Colaleo^a, D. Creanza^{a,c}, L. Cristella^{a,b}, N. De Filippis^{a,c}, M. De Palma^{a,b}, L. Fiore^a, G. Iaselli^{a,c}, G. Maggi^{a,c}, M. Maggi^a, G. Miniello^{a,b}, S. My^{a,b}, S. Nuzzo^{a,b}, A. Pompili^{a,b}, G. Pugliese^{a,c}, R. Radogna^{a,b}, A. Ranieri^a, G. Selvaggi^{a,b}, L. Silvestris^{a,15}, R. Venditti^{a,b}, P. Verwilligen^a

INFN Sezione di Bologna ^a, Università di Bologna ^b, Bologna, Italy

G. Abbiendi^a, C. Battilana, D. Bonacorsi^{a,b}, S. Braibant-Giacomelli^{a,b}, L. Brigliadori^{a,b}, R. Campanini^{a,b}, P. Capiluppi^{a,b}, A. Castro^{a,b}, F.R. Cavallo^a, S.S. Chhibra^{a,b}, G. Codispoti^{a,b}, M. Cuffiani^{a,b}, G.M. Dallavalle^a, F. Fabbri^a, A. Fanfani^{a,b}, D. Fasanella^{a,b}, P. Giacomelli^a, C. Grandi^a, L. Guiducci^{a,b}, S. Marcellini^a, G. Masetti^a, A. Montanari^a, F.L. Navarria^{a,b}, A. Perrotta^a, A.M. Rossi^{a,b}, T. Rovelli^{a,b}, G.P. Siroli^{a,b}, N. Tosi^{a,b,15}

INFN Sezione di Catania ^a, Università di Catania ^b, Catania, Italy

S. Albergo^{a,b}, M. Chiorboli^{a,b}, S. Costa^{a,b}, A. Di Mattia^a, F. Giordano^{a,b}, R. Potenza^{a,b}, A. Tricomi^{a,b}, C. Tuve^{a,b}

INFN Sezione di Firenze ^a, Università di Firenze ^b, Firenze, Italy

G. Barbagli^a, V. Ciulli^{a,b}, C. Civinini^a, R. D'Alessandro^{a,b}, E. Focardi^{a,b}, V. Gori^{a,b}, P. Lenzi^{a,b}, M. Meschini^a, S. Paoletti^a, G. Sguazzoni^a, L. Viliani^{a,b,15}

INFN Laboratori Nazionali di Frascati, Frascati, Italy

L. Benussi, S. Bianco, F. Fabbri, D. Piccolo, F. Primavera¹⁵

INFN Sezione di Genova ^a, Università di Genova ^b, Genova, Italy

V. Calvelli^{a,b}, F. Ferro^a, M. Lo Vetere^{a,b}, M.R. Monge^{a,b}, E. Robutti^a, S. Tosi^{a,b}

INFN Sezione di Milano-Bicocca ^a, Università di Milano-Bicocca ^b, Milano, Italy

L. Brianza, M.E. Dinardo^{a,b}, S. Fiorendi^{a,b}, S. Gennai^a, A. Ghezzi^{a,b}, P. Govoni^{a,b}, S. Malvezzi^a, R.A. Manzoni^{a,b,15}, B. Marzocchi^{a,b}, D. Menasce^a, L. Moroni^a, M. Paganoni^{a,b}, D. Pedrini^a, S. Pigazzini, S. Ragazzi^{a,b}, T. Tabarelli de Fatis^{a,b}

INFN Sezione di Napoli ^a, Università di Napoli 'Federico II' ^b, Napoli, Italy, Università della Basilicata ^c, Potenza, Italy, Università G. Marconi ^d, Roma, Italy

S. Buontempo^a, N. Cavallo^{a,c}, G. De Nardo, S. Di Guida^{a,d,15}, M. Esposito^{a,b}, F. Fabozzi^{a,c}, A.O.M. Iorio^{a,b}, G. Lanza^a, L. Lista^a, S. Meola^{a,d,15}, M. Merola^a, P. Paolucci^{a,15}, C. Sciacca^{a,b}, F. Thyssen

INFN Sezione di Padova ^a, Università di Padova ^b, Padova, Italy, Università di Trento ^c, Trento, Italy

P. Azzi^{a,15}, N. Bacchetta^a, L. Benato^{a,b}, M. Biasotto^{a,30}, A. Boletti^{a,b}, A. Carvalho Antunes De Oliveira^{a,b}, M. Dall'Osso^{a,b}, P. De Castro Manzano^a, T. Dorigo^a, U. Dosselli^a, S. Fantinel^a, F. Fanzago^a, F. Gasparini^{a,b}, U. Gasparini^{a,b}, M. Gulmini^{a,30}, S. Lacaprara^a, M. Margoni^{a,b}, A.T. Meneguzzo^{a,b}, J. Pazzini^{a,b,15}, N. Pozzobon^{a,b}, P. Ronchese^{a,b}, E. Torassa^a, S. Ventura^a, M. Zanetti, P. Zotto^{a,b}, A. Zucchetta^{a,b}, G. Zumerle^{a,b}

INFN Sezione di Pavia ^a, Università di Pavia ^b, Pavia, Italy

A. Braghieri^a, A. Magnani^{a,b}, P. Montagna^{a,b}, S.P. Ratti^{a,b}, V. Re^a, C. Riccardi^{a,b}, P. Salvini^a, I. Vai^{a,b}, P. Vitulo^{a,b}

INFN Sezione di Perugia ^a, Università di Perugia ^b, Perugia, Italy

L. Alunni Solestizi^{a,b}, G.M. Bilei^a, D. Ciangottini^{a,b}, L. Fanò^{a,b}, P. Lariccia^{a,b}, R. Leonardi^{a,b}, G. Mantovani^{a,b}, M. Menichelli^a, A. Saha^a, A. Santocchia^{a,b}

INFN Sezione di Pisa ^a, Università di Pisa ^b, Scuola Normale Superiore di Pisa ^c, Pisa, Italy

K. Androsov^{a,31}, P. Azzurri^{a,15}, G. Bagliesi^a, J. Bernardini^a, T. Boccali^a, R. Castaldi^a, M.A. Ciocci^{a,31}, R. Dell'Orso^a, S. Donato^{a,c}, G. Fedi, A. Giassi^a, M.T. Grippo^{a,31}, F. Ligabue^{a,c}, T. Lomtadze^a, L. Martini^{a,b}, A. Messineo^{a,b}, F. Palla^a, A. Rizzi^{a,b}, A. Savoy-Navarro^{a,32}, P. Spagnolo^a, R. Tenchini^a, G. Tonelli^{a,b}, A. Venturi^a, P.G. Verdini^a

INFN Sezione di Roma ^a, Università di Roma ^b, Roma, Italy

L. Barone^{a,b}, F. Cavallari^a, M. Cipriani^{a,b}, G. D'imperio^{a,b,15}, D. Del Re^{a,b,15}, M. Diemoz^a, S. Gelli^{a,b}, C. Jorda^a, E. Longo^{a,b}, F. Margaroli^{a,b}, P. Meridiani^a, G. Organtini^{a,b}, R. Paramatti^a, F. Preiato^{a,b}, S. Rahatlou^{a,b}, C. Rovelli^a, F. Santanastasio^{a,b}

INFN Sezione di Torino ^a, Università di Torino ^b, Torino, Italy, Università del Piemonte Orientale ^c, Novara, Italy

N. Amapane^{a,b}, R. Arcidiacono^{a,c,15}, S. Argiro^{a,b}, M. Arneodo^{a,c}, N. Bartosik^a, R. Bellan^{a,b}, C. Biino^a, N. Cartiglia^a, F. Cenna^{a,b}, M. Costa^{a,b}, R. Covarelli^{a,b}, A. Degano^{a,b}, N. Demaria^a, L. Finco^{a,b}, B. Kiani^{a,b}, C. Mariotti^a, S. Maselli^a, E. Migliore^{a,b}, V. Monaco^{a,b}, E. Monteil^{a,b}, M.M. Obertino^{a,b}, L. Pacher^{a,b}, N. Pastrone^a, M. Pelliccioni^a, G.L. Pinna Angioni^{a,b}, F. Ravera^{a,b}

A. Romero^{a,b}, M. Ruspa^{a,c}, R. Sacchi^{a,b}, K. Shchelina^{a,b}, V. Sola^a, A. Solano^{a,b}, A. Staiano^a, P. Traczyk^{a,b}

INFN Sezione di Trieste ^a, Università di Trieste ^b, Trieste, Italy

S. Belforte^a, M. Casarsa^a, F. Cossutti^a, G. Della Ricca^{a,b}, C. La Licata^{a,b}, A. Schizzi^{a,b}, A. Zanetti^a

Kyungpook National University, Daegu, Korea

D.H. Kim, G.N. Kim, M.S. Kim, S. Lee, S.W. Lee, Y.D. Oh, S. Sekmen, D.C. Son, Y.C. Yang

Chonbuk National University, Jeonju, Korea

H. Kim, A. Lee

Hanyang University, Seoul, Korea

J.A. Brochero Cifuentes, T.J. Kim

Korea University, Seoul, Korea

S. Cho, S. Choi, Y. Go, D. Gyun, S. Ha, B. Hong, Y. Jo, Y. Kim, B. Lee, K. Lee, K.S. Lee, S. Lee, J. Lim, S.K. Park, Y. Roh

Seoul National University, Seoul, Korea

J. Almond, J. Kim, S.B. Oh, S.h. Seo, U.K. Yang, H.D. Yoo, G.B. Yu

University of Seoul, Seoul, Korea

M. Choi, H. Kim, H. Kim, J.H. Kim, J.S.H. Lee, I.C. Park, G. Ryu, M.S. Ryu

Sungkyunkwan University, Suwon, Korea

Y. Choi, J. Goh, C. Hwang, D. Kim, J. Lee, I. Yu

Vilnius University, Vilnius, Lithuania

V. Dudenas, A. Juodagalvis, J. Vaitkus

National Centre for Particle Physics, Universiti Malaya, Kuala Lumpur, Malaysia

I. Ahmed, Z.A. Ibrahim, J.R. Komaragiri, M.A.B. Md Ali³³, F. Mohamad Idris³⁴, W.A.T. Wan Abdullah, M.N. Yusli, Z. Zolkapli

Centro de Investigacion y de Estudios Avanzados del IPN, Mexico City, Mexico

H. Castilla-Valdez, E. De La Cruz-Burelo, I. Heredia-De La Cruz³⁵, A. Hernandez-Almada, R. Lopez-Fernandez, J. Mejia Guisao, A. Sanchez-Hernandez

Universidad Iberoamericana, Mexico City, Mexico

S. Carrillo Moreno, C. Oropeza Barrera, F. Vazquez Valencia

Benemerita Universidad Autonoma de Puebla, Puebla, Mexico

S. Carpintero, I. Pedraza, H.A. Salazar Ibarguen, C. Uribe Estrada

Universidad Autónoma de San Luis Potosí, San Luis Potosí, Mexico

A. Morelos Pineda

University of Auckland, Auckland, New Zealand

D. Kofcheck

University of Canterbury, Christchurch, New Zealand

P.H. Butler

National Centre for Physics, Quaid-I-Azam University, Islamabad, Pakistan

A. Ahmad, M. Ahmad, Q. Hassan, H.R. Hoorani, W.A. Khan, M.A. Shah, M. Shoaib, M. Waqas

National Centre for Nuclear Research, Swierk, Poland

H. Bialkowska, M. Bluj, B. Boimska, T. Frueboes, M. Górski, M. Kazana, K. Nawrocki, K. Romanowska-Rybinska, M. Szleper, P. Zalewski

Institute of Experimental Physics, Faculty of Physics, University of Warsaw, Warsaw, Poland

K. Bunkowski, A. Byszuk³⁶, K. Doroba, A. Kalinowski, M. Konecki, J. Krolikowski, M. Misiura, M. Olszewski, M. Walczak

Laboratório de Instrumentação e Física Experimental de Partículas, Lisboa, Portugal

P. Bargassa, C. Beirão Da Cruz E Silva, A. Di Francesco, P. Faccioli, P.G. Ferreira Parracho, M. Gallinaro, J. Hollar, N. Leonardo, L. Lloret Iglesias, M.V. Nemallapudi, J. Rodrigues Antunes, J. Seixas, O. Toldaiev, D. Vadruccio, J. Varela, P. Vischia

Joint Institute for Nuclear Research, Dubna, Russia

S. Afanasiev, P. Bunin, I. Golutvin, V. Karjavin, V. Korenkov, A. Lanev, A. Malakhov, V. Matveev^{37,38}, V.V. Mitsyn, P. Moisenz, V. Palichik, V. Perelygin, S. Shmatov, S. Shulha, N. Skatchkov, V. Smirnov, E. Tikhonenko, N. Voytishin, A. Zarubin

Petersburg Nuclear Physics Institute, Gatchina (St. Petersburg), Russia

L. Chtchipounov, V. Golovtsov, Y. Ivanov, V. Kim³⁹, E. Kuznetsova⁴⁰, V. Murzin, V. Oreshkin, V. Sulimov, A. Vorobyev

Institute for Nuclear Research, Moscow, Russia

Yu. Andreev, A. Dermenev, S. Gninenko, N. Golubev, A. Karneyeu, M. Kirsanov, N. Krasnikov, A. Pashenkov, D. Tlisov, A. Toropin

Institute for Theoretical and Experimental Physics, Moscow, Russia

V. Epshteyn, V. Gavrilov, N. Lychkovskaya, V. Popov, I. Pozdnyakov, G. Safronov, A. Spiridonov, M. Toms, E. Vlasov, A. Zhokin

National Research Nuclear University 'Moscow Engineering Physics Institute' (MEPhI), Moscow, Russia

R. Chistov⁴¹, V. Rusinov, E. Tarkovskii

P.N. Lebedev Physical Institute, Moscow, Russia

V. Andreev, M. Azarkin³⁸, I. Dremin³⁸, M. Kirakosyan, A. Leonidov³⁸, S.V. Rusakov, A. Terkulov

Skobeltsyn Institute of Nuclear Physics, Lomonosov Moscow State University, Moscow, Russia

A. Baskakov, A. Belyaev, E. Boos, M. Dubinin⁴², L. Dudko, A. Ershov, A. Gribushin, V. Klyukhin, O. Kodolova, I. Lokhtin, I. Miagkov, S. Obraztsov, S. Petrushanko, V. Savrin, A. Snigirev

State Research Center of Russian Federation, Institute for High Energy Physics, Protvino, Russia

I. Azhgirey, I. Bayshev, S. Bitioukov, D. Elumakhov, V. Kachanov, A. Kalinin, D. Konstantinov, V. Krychkine, V. Petrov, R. Ryutin, A. Sobol, S. Troshin, N. Tyurin, A. Uzunian, A. Volkov

University of Belgrade, Faculty of Physics and Vinca Institute of Nuclear Sciences, Belgrade, Serbia

P. Adzic⁴³, P. Cirkovic, D. Devetak, J. Milosevic, V. Rekovic

Centro de Investigaciones Energéticas Medioambientales y Tecnológicas (CIEMAT), Madrid, Spain

J. Alcaraz Maestre, E. Calvo, M. Cerrada, M. Chamizo Llatas, N. Colino, B. De La Cruz, A. Delgado Peris, A. Escalante Del Valle, C. Fernandez Bedoya, J.P. Fernández Ramos, J. Flix, M.C. Fouz, P. Garcia-Abia, O. Gonzalez Lopez, S. Goy Lopez, J.M. Hernandez, M.I. Josa, E. Navarro De Martino, A. Pérez-Calero Yzquierdo, J. Puerta Pelayo, A. Quintario Olmeda, I. Redondo, L. Romero, M.S. Soares

Universidad Autónoma de Madrid, Madrid, Spain

J.F. de Trocóniz, M. Missiroli, D. Moran

Universidad de Oviedo, Oviedo, Spain

J. Cuevas, J. Fernandez Menendez, I. Gonzalez Caballero, J.R. González Fernández, E. Palencia Cortezon, S. Sanchez Cruz, J.M. Vizan Garcia

Instituto de Física de Cantabria (IFCA), CSIC-Universidad de Cantabria, Santander, Spain

I.J. Cabrillo, A. Calderon, J.R. Castiñeiras De Saa, E. Curras, M. Fernandez, J. Garcia-Ferrero, G. Gomez, A. Lopez Virto, J. Marco, C. Martinez Rivero, F. Matorras, J. Piedra Gomez, T. Rodrigo, A. Ruiz-Jimeno, L. Scodellaro, N. Trevisani, I. Vila, R. Vilar Cortabitarte

CERN, European Organization for Nuclear Research, Geneva, Switzerland

D. Abbaneo, E. Auffray, G. Auzinger, M. Bachtis, P. Baillon, A.H. Ball, D. Barney, P. Bloch, A. Bocci, A. Bonato, C. Botta, T. Camporesi, R. Castello, M. Cepeda, G. Cerminara, M. D'Alfonso, D. d'Enterria, A. Dabrowski, V. Daponte, A. David, M. De Gruttola, F. De Guio, A. De Roeck, E. Di Marco⁴⁴, M. Dobson, M. Dordevic, B. Dorney, T. du Pree, D. Duggan, M. Dünser, N. Dupont, A. Elliott-Peisert, S. Fartoukh, G. Franzoni, J. Fulcher, W. Funk, D. Gigi, K. Gill, M. Girone, F. Glege, D. Gulhan, S. Gundacker, M. Guthoff, J. Hammer, P. Harris, J. Hegeman, V. Innocente, P. Janot, H. Kirschenmann, V. Knünz, M.J. Kortelainen, K. Kousouris, M. Krammer¹, P. Lecoq, C. Lourenço, M.T. Lucchini, L. Malgeri, M. Mannelli, A. Martelli, F. Meijers, S. Mersi, E. Meschi, F. Moortgat, S. Morovic, M. Mulders, H. Neugebauer, S. Orfanelli⁴⁵, L. Orsini, L. Pape, E. Perez, M. Peruzzi, A. Petrilli, G. Petrucciani, A. Pfeiffer, M. Pierini, A. Racz, T. Reis, G. Rolandi⁴⁶, M. Rovere, M. Ruan, H. Sakulin, J.B. Sauvan, C. Schäfer, C. Schwick, M. Seidel, A. Sharma, P. Silva, M. Simon, P. Sphicas⁴⁷, J. Steggemann, M. Stoye, Y. Takahashi, M. Tosi, D. Treille, A. Triossi, A. Tsirou, V. Veckalns⁴⁸, G.I. Veres²¹, N. Wardle, H.K. Wöhri, A. Zagozdzinska³⁶, W.D. Zeuner

Paul Scherrer Institut, Villigen, Switzerland

W. Bertl, K. Deiters, W. Erdmann, R. Horisberger, Q. Ingram, H.C. Kaestli, D. Kotlinski, U. Langenegger, T. Rohe

Institute for Particle Physics, ETH Zurich, Zurich, Switzerland

F. Bachmair, L. Bäni, L. Bianchini, B. Casal, G. Dissertori, M. Dittmar, M. Donegà, P. Eller, C. Grab, C. Heidegger, D. Hits, J. Hoss, G. Kasieczka, P. Lecomte[†], W. Lustermann, B. Mangano, M. Marionneau, P. Martinez Ruiz del Arbol, M. Masciovecchio, M.T. Meinhard, D. Meister, F. Micheli, P. Musella, F. Nessi-Tedaldi, F. Pandolfi, J. Pata, F. Pauss, G. Perrin, L. Perrozzi, M. Quitnat, M. Rossini, M. Schönenberger, A. Starodumov⁴⁹, M. Takahashi, V.R. Tavolaro, K. Theofilatos, R. Wallny

Universität Zürich, Zurich, Switzerland

T.K. Arrestad, C. Amsler⁵⁰, L. Caminada, M.F. Canelli, V. Chiochia, A. De Cosa, C. Galloni, A. Hinzmann, T. Hreus, B. Kilminster, C. Lange, J. Ngadiuba, D. Pinna, G. Rauco, P. Robmann, D. Salerno, Y. Yang

National Central University, Chung-Li, Taiwan

V. Candelise, T.H. Doan, Sh. Jain, R. Khurana, M. Konyushikhin, C.M. Kuo, W. Lin, Y.J. Lu, A. Pozdnyakov, S.S. Yu

National Taiwan University (NTU), Taipei, Taiwan

Arun Kumar, P. Chang, Y.H. Chang, Y.W. Chang, Y. Chao, K.F. Chen, P.H. Chen, C. Dietz, F. Fiori, W.-S. Hou, Y. Hsiung, Y.F. Liu, R.-S. Lu, M. Miñano Moya, E. Paganis, A. Psallidas, J.f. Tsai, Y.M. Tzeng

Chulalongkorn University, Faculty of Science, Department of Physics, Bangkok, Thailand

B. Asavapibhop, G. Singh, N. Srimanobhas, N. Suwonjandee

Cukurova University, Adana, Turkey

A. Adiguzel, S. Cerci⁵¹, S. Damarseckin, Z.S. Demiroglu, C. Dozen, I. Dumanoglu, S. Girgis, G. Gokbulut, Y. Guler, E. Gurpinar, I. Hos, E.E. Kangal⁵², O. Kara, A. Kayis Topaksu, U. Kiminsu, M. Oglakci, G. Onengut⁵³, K. Ozdemir⁵⁴, D. Sunar Cerci⁵¹, H. Topakli⁵⁵, S. Turkcapar, I.S. Zorbakir, C. Zorbilmez

Middle East Technical University, Physics Department, Ankara, Turkey

B. Bilin, S. Bilmis, B. Isildak⁵⁶, G. Karapinar⁵⁷, M. Yalvac, M. Zeyrek

Bogazici University, Istanbul, Turkey

E. Gülmез, M. Kaya⁵⁸, O. Kaya⁵⁹, E.A. Yetkin⁶⁰, T. Yetkin⁶¹

Istanbul Technical University, Istanbul, Turkey

A. Cakir, K. Cankocak, S. Sen⁶²

Institute for Scintillation Materials of National Academy of Science of Ukraine, Kharkov, Ukraine

B. Grynyov

National Scientific Center, Kharkov Institute of Physics and Technology, Kharkov, Ukraine

L. Levchuk, P. Sorokin

University of Bristol, Bristol, United Kingdom

R. Aggleton, F. Ball, L. Beck, J.J. Brooke, D. Burns, E. Clement, D. Cussans, H. Flacher, J. Goldstein, M. Grimes, G.P. Heath, H.F. Heath, J. Jacob, L. Kreczko, C. Lucas, D.M. Newbold⁶³, S. Paramesvaran, A. Poll, T. Sakuma, S. Seif El Nasr-storey, D. Smith, V.J. Smith

Rutherford Appleton Laboratory, Didcot, United Kingdom

K.W. Bell, A. Belyaev⁶⁴, C. Brew, R.M. Brown, L. Calligaris, D. Cieri, D.J.A. Cockerill, J.A. Coughlan, K. Harder, S. Harper, E. Olaiya, D. Petyt, C.H. Shepherd-Themistocleous, A. Thea, I.R. Tomalin, T. Williams

Imperial College, London, United Kingdom

M. Baber, R. Bainbridge, O. Buchmuller, A. Bundock, D. Burton, S. Casasso, M. Citron, D. Colling, L. Corpe, P. Dauncey, G. Davies, A. De Wit, M. Della Negra, P. Dunne, A. Elwood, D. Futyan, Y. Haddad, G. Hall, G. Iles, R. Lane, C. Laner, R. Lucas⁶³, L. Lyons, A.-M. Magnan, S. Malik, L. Mastrolorenzo, J. Nash, A. Nikitenko⁴⁹, J. Pela, B. Penning, M. Pesaresi, D.M. Raymond, A. Richards, A. Rose, C. Seez, A. Tapper, K. Uchida, M. Vazquez Acosta⁶⁵, T. Virdee¹⁵, S.C. Zenz

Brunel University, Uxbridge, United Kingdom

J.E. Cole, P.R. Hobson, A. Khan, P. Kyberd, D. Leslie, I.D. Reid, P. Symonds, L. Teodorescu, M. Turner

Baylor University, Waco, USA

A. Borzou, K. Call, J. Dittmann, K. Hatakeyama, H. Liu, N. Pastika

The University of Alabama, Tuscaloosa, USA

O. Charaf, S.I. Cooper, C. Henderson, P. Rumerio

Boston University, Boston, USA

D. Arcaro, A. Avetisyan, T. Bose, D. Gastler, D. Rankin, C. Richardson, J. Rohlf, L. Sulak, D. Zou

Brown University, Providence, USA

G. Benelli, E. Berry, D. Cutts, A. Garabedian, J. Hakala, U. Heintz, O. Jesus, E. Laird, G. Landsberg, Z. Mao, M. Narain, S. Piperov, S. Sagir, E. Spencer, R. Syarif

University of California, Davis, Davis, USA

R. Breedon, G. Breto, D. Burns, M. Calderon De La Barca Sanchez, S. Chauhan, M. Chertok, J. Conway, R. Conway, P.T. Cox, R. Erbacher, C. Flores, G. Funk, M. Gardner, W. Ko, R. Lander, C. Mclean, M. Mulhearn, D. Pellett, J. Pilot, F. Ricci-Tam, S. Shalhout, J. Smith, M. Squires, D. Stolp, M. Tripathi, S. Wilbur, R. Yohay

University of California, Los Angeles, USA

R. Cousins, P. Everaerts, A. Florent, J. Hauser, M. Ignatenko, D. Saltzberg, E. Takasugi, V. Valuev, M. Weber

University of California, Riverside, Riverside, USA

K. Burt, R. Clare, J. Ellison, J.W. Gary, G. Hanson, J. Heilman, P. Jandir, E. Kennedy, F. Lacroix, O.R. Long, M. Malberti, M. Olmedo Negrete, M.I. Paneva, A. Shrinivas, H. Wei, S. Wimpenny, B. R. Yates

University of California, San Diego, La Jolla, USA

J.G. Branson, G.B. Cerati, S. Cittolin, M. Derdzinski, R. Gerosa, A. Holzner, D. Klein, J. Letts, I. Macneill, D. Olivito, S. Padhi, M. Pieri, M. Sani, V. Sharma, S. Simon, M. Tadel, A. Vartak, S. Wasserbaech⁶⁶, C. Welke, J. Wood, F. Würthwein, A. Yagil, G. Zevi Della Porta

University of California, Santa Barbara - Department of Physics, Santa Barbara, USA

R. Bhandari, J. Bradmiller-Feld, C. Campagnari, A. Dishaw, V. Dutta, K. Flowers, M. Franco Sevilla, P. Geffert, C. George, F. Golf, L. Gouskos, J. Gran, R. Heller, J. Incandela, N. Mccoll, S.D. Mullin, A. Ovcharova, J. Richman, D. Stuart, I. Suarez, C. West, J. Yoo

California Institute of Technology, Pasadena, USA

D. Anderson, A. Apresyan, J. Bendavid, A. Bornheim, J. Bunn, Y. Chen, J. Duarte, A. Mott, H.B. Newman, C. Pena, M. Spiropulu, J.R. Vlimant, S. Xie, R.Y. Zhu

Carnegie Mellon University, Pittsburgh, USA

M.B. Andrews, V. Azzolini, B. Carlson, T. Ferguson, M. Paulini, J. Russ, M. Sun, H. Vogel, I. Vorobiev

University of Colorado Boulder, Boulder, USA

J.P. Cumalat, W.T. Ford, F. Jensen, A. Johnson, M. Krohn, T. Mulholland, K. Stenson, S.R. Wagner

Cornell University, Ithaca, USA

J. Alexander, J. Chaves, J. Chu, S. Dittmer, N. Mirman, G. Nicolas Kaufman, J.R. Patterson, A. Rinkevicius, A. Ryd, L. Skinnari, S.M. Tan, Z. Tao, J. Thom, J. Tucker, P. Wittich

Fairfield University, Fairfield, USA

D. Winn

Fermi National Accelerator Laboratory, Batavia, USA

S. Abdullin, M. Albrow, G. Apollinari, S. Banerjee, L.A.T. Bauerick, A. Beretvas, J. Berryhill, P.C. Bhat, G. Bolla, K. Burkett, J.N. Butler, H.W.K. Cheung, F. Chlebana, S. Cihangir, M. Cremonesi, V.D. Elvira, I. Fisk, J. Freeman, E. Gottschalk, L. Gray, D. Green, S. Grünendahl, O. Gutsche, D. Hare, R.M. Harris, S. Hasegawa, J. Hirschauer, Z. Hu, B. Jayatilaka, S. Jindariani, M. Johnson, U. Joshi, B. Klima, B. Kreis, S. Lammel, J. Linacre, D. Lincoln, R. Lipton, T. Liu, R. Lopes De Sá, J. Lykken, K. Maeshima, N. Magini, J.M. Marraffino, S. Maruyama, D. Mason, P. McBride, P. Merkel, S. Mrenna, S. Nahm, C. Newman-Holmes[†], V. O'Dell, K. Pedro, O. Prokofyev, G. Rakness, L. Ristori, E. Sexton-Kennedy, A. Soha, W.J. Spalding, L. Spiegel, S. Stoynev, N. Strobbe, L. Taylor, S. Tkaczyk, N.V. Tran, L. Uplegger, E.W. Vaandering, C. Vernieri, M. Verzocchi, R. Vidal, M. Wang, H.A. Weber, A. Whitbeck

University of Florida, Gainesville, USA

D. Acosta, P. Avery, P. Bortignon, D. Bourilkov, A. Brinkerhoff, A. Carnes, M. Carver, D. Curry, S. Das, R.D. Field, I.K. Furic, J. Konigsberg, A. Korytov, P. Ma, K. Matchev, H. Mei, P. Milenovic⁶⁷, G. Mitselmakher, D. Rank, L. Shchutska, D. Sperka, L. Thomas, J. Wang, S. Wang, J. Yelton

Florida International University, Miami, USA

S. Linn, P. Markowitz, G. Martinez, J.L. Rodriguez

Florida State University, Tallahassee, USA

A. Ackert, J.R. Adams, T. Adams, A. Askew, S. Bein, B. Diamond, S. Hagopian, V. Hagopian, K.F. Johnson, A. Khatiwada, H. Prosper, A. Santra, M. Weinberg

Florida Institute of Technology, Melbourne, USA

M.M. Baarmand, V. Bhopatkar, S. Colafranceschi⁶⁸, M. Hohlmann, D. Noonan, T. Roy, F. Yumiceva

University of Illinois at Chicago (UIC), Chicago, USA

M.R. Adams, L. Apanasevich, D. Berry, R.R. Betts, I. Bucinskaite, R. Cavanaugh, O. Evdokimov, L. Gauthier, C.E. Gerber, D.J. Hofman, P. Kurt, C. O'Brien, I.D. Sandoval Gonzalez, P. Turner, N. Varelas, Z. Wu, M. Zakaria, J. Zhang

The University of Iowa, Iowa City, USA

B. Bilki⁶⁹, W. Clarida, K. Dilisiz, S. Durgut, R.P. Gandrajula, M. Haytmyradov, V. Khristenko, J.-P. Merlo, H. Mermerkaya⁷⁰, A. Mestvirishvili, A. Moeller, J. Nachtman, H. Ogul, Y. Onel, F. Ozok⁷¹, A. Penzo, C. Snyder, E. Tiras, J. Wetzel, K. Yi

Johns Hopkins University, Baltimore, USA

I. Anderson, B. Blumenfeld, A. Cocoros, N. Eminizer, D. Fehling, L. Feng, A.V. Gritsan, P. Maksimovic, M. Osherson, J. Roskes, U. Sarica, M. Swartz, M. Xiao, Y. Xin, C. You

The University of Kansas, Lawrence, USA

A. Al-bataineh, P. Baringer, A. Bean, J. Bowen, C. Bruner, J. Castle, R.P. Kenny III, A. Kropivnitskaya, D. Majumder, W. Mcbrayer, M. Murray, S. Sanders, R. Stringer, J.D. Tapia Takaki, Q. Wang

Kansas State University, Manhattan, USA

A. Ivanov, K. Kaadze, S. Khalil, M. Makouski, Y. Maravin, A. Mohammadi, L.K. Saini, N. Skhirtladze, S. Toda

Lawrence Livermore National Laboratory, Livermore, USA

D. Lange, F. Rebassoo, D. Wright

University of Maryland, College Park, USA

C. Anelli, A. Baden, O. Baron, A. Belloni, B. Calvert, S.C. Eno, C. Ferraioli, J.A. Gomez, N.J. Hadley, S. Jabeen, R.G. Kellogg, T. Kolberg, J. Kunkle, Y. Lu, A.C. Mignerey, Y.H. Shin, A. Skuja, M.B. Tonjes, S.C. Tonwar

Massachusetts Institute of Technology, Cambridge, USA

A. Apyan, R. Barbieri, A. Baty, R. Bi, K. Bierwagen, S. Brandt, W. Busza, I.A. Cali, Z. Demiragli, L. Di Matteo, G. Gomez Ceballos, M. Goncharov, D. Hsu, Y. Iiyama, G.M. Innocenti, M. Klute, D. Kovalevskyi, K. Krajczar, Y.S. Lai, Y.-J. Lee, A. Levin, P.D. Luckey, A.C. Marini, C. McGinn, C. Mironov, S. Narayanan, X. Niu, C. Paus, C. Roland, G. Roland, J. Salfeld-Nebgen, G.S.F. Stephans, K. Sumorok, K. Tatar, M. Varma, D. Velicanu, J. Veverka, J. Wang, T.W. Wang, B. Wyslouch, M. Yang, V. Zhukova

University of Minnesota, Minneapolis, USA

A.C. Benvenuti, R.M. Chatterjee, A. Evans, A. Finkel, A. Gude, P. Hansen, S. Kalafut, S.C. Kao, Y. Kubota, Z. Lesko, J. Mans, S. Nourbakhsh, N. Ruckstuhl, R. Rusack, N. Tambe, J. Turkewitz

University of Mississippi, Oxford, USA

J.G. Acosta, S. Oliveros

University of Nebraska-Lincoln, Lincoln, USA

E. Avdeeva, R. Bartek, K. Bloom, S. Bose, D.R. Claes, A. Dominguez, C. Fangmeier, R. Gonzalez Suarez, R. Kamalieddin, D. Knowlton, I. Kravchenko, A. Malta Rodrigues, F. Meier, J. Monroy, J.E. Siado, G.R. Snow, B. Stieger

State University of New York at Buffalo, Buffalo, USA

M. Alyari, J. Dolen, J. George, A. Godshalk, C. Harrington, I. Iashvili, J. Kaisen, A. Kharchilava, A. Kumar, A. Parker, S. Rappoccio, B. Roozbahani

Northeastern University, Boston, USA

G. Alverson, E. Barberis, D. Baumgartel, M. Chasco, A. Hortiangtham, A. Massironi, D.M. Morse, D. Nash, T. Orimoto, R. Teixeira De Lima, D. Trocino, R.-J. Wang, D. Wood

Northwestern University, Evanston, USA

S. Bhattacharya, K.A. Hahn, A. Kubik, J.F. Low, N. Mucia, N. Odell, B. Pollack, M.H. Schmitt, K. Sung, M. Trovato, M. Velasco

University of Notre Dame, Notre Dame, USA

N. Dev, M. Hildreth, K. Hurtado Anampa, C. Jessop, D.J. Karmgard, N. Kellams, K. Lannon, N. Marinelli, F. Meng, C. Mueller, Y. Musienko³⁷, M. Planer, A. Reinsvold, R. Ruchti, G. Smith, S. Taroni, N. Valls, M. Wayne, M. Wolf, A. Woodard

The Ohio State University, Columbus, USA

J. Alimena, L. Antonelli, J. Brinson, B. Bylsma, L.S. Durkin, S. Flowers, B. Francis, A. Hart, C. Hill, R. Hughes, W. Ji, B. Liu, W. Luo, D. Puigh, B.L. Winer, H.W. Wulsin

Princeton University, Princeton, USA

S. Cooperstein, O. Driga, P. Elmer, J. Hardenbrook, P. Hebda, J. Luo, D. Marlow, T. Medvedeva, M. Mooney, J. Olsen, C. Palmer, P. Piroué, D. Stickland, C. Tully, A. Zuranski

University of Puerto Rico, Mayaguez, USA

S. Malik

Purdue University, West Lafayette, USA

A. Barker, V.E. Barnes, D. Benedetti, S. Folgueras, L. Gutay, M.K. Jha, M. Jones, A.W. Jung,

K. Jung, D.H. Miller, N. Neumeister, B.C. Radburn-Smith, X. Shi, J. Sun, A. Svyatkovskiy, F. Wang, W. Xie, L. Xu

Purdue University Calumet, Hammond, USA

N. Parashar, J. Stupak

Rice University, Houston, USA

A. Adair, B. Akgun, Z. Chen, K.M. Ecklund, F.J.M. Geurts, M. Guilbaud, W. Li, B. Michlin, M. Northup, B.P. Padley, R. Redjimi, J. Roberts, J. Rorie, Z. Tu, J. Zabel

University of Rochester, Rochester, USA

B. Betchart, A. Bodek, P. de Barbaro, R. Demina, Y.t. Duh, T. Ferbel, M. Galanti, A. Garcia-Bellido, J. Han, O. Hindrichs, A. Khukhunaishvili, K.H. Lo, P. Tan, M. Verzetti

The Rockefeller University, New York, USA

C. Mesropian

Rutgers, The State University of New Jersey, Piscataway, USA

J.P. Chou, E. Contreras-Campana, Y. Gershtein, T.A. Gómez Espinosa, E. Halkiadakis, M. Heindl, D. Hidas, E. Hughes, S. Kaplan, R. Kunawalkam Elayavalli, S. Kyriacou, A. Lath, K. Nash, H. Saka, S. Salur, S. Schnetzer, D. Sheffield, S. Somalwar, R. Stone, S. Thomas, P. Thomassen, M. Walker

University of Tennessee, Knoxville, USA

M. Foerster, J. Heideman, G. Riley, K. Rose, S. Spanier, K. Thapa

Texas A&M University, College Station, USA

O. Bouhali⁷², A. Celik, M. Dalchenko, M. De Mattia, A. Delgado, S. Dildick, R. Eusebi, J. Gilmore, T. Huang, E. Juska, T. Kamon⁷³, V. Krutelyov, R. Mueller, Y. Pakhotin, R. Patel, A. Perloff, L. Perniè, D. Rathjens, A. Rose, A. Safonov, A. Tatarinov, K.A. Ulmer

Texas Tech University, Lubbock, USA

N. Akchurin, C. Cowden, J. Damgov, C. Dragoiu, P.R. Dudero, J. Faulkner, S. Kunori, K. Lamichhane, S.W. Lee, T. Libeiro, S. Undleeb, I. Volobouev, Z. Wang

Vanderbilt University, Nashville, USA

A.G. Delannoy, S. Greene, A. Gurrola, R. Janjam, W. Johns, C. Maguire, A. Melo, H. Ni, P. Sheldon, S. Tuo, J. Velkovska, Q. Xu

University of Virginia, Charlottesville, USA

M.W. Arenton, P. Barria, B. Cox, J. Goodell, R. Hirosky, A. Ledovskoy, H. Li, C. Neu, T. Sinhuprasith, X. Sun, Y. Wang, E. Wolfe, F. Xia

Wayne State University, Detroit, USA

C. Clarke, R. Harr, P.E. Karchin, P. Lamichhane, J. Sturdy

University of Wisconsin - Madison, Madison, WI, USA

D.A. Belknap, S. Dasu, L. Dodd, S. Duric, B. Gomber, M. Grothe, M. Herndon, A. Hervé, P. Klabbers, A. Lanaro, A. Levine, K. Long, R. Loveless, I. Ojalvo, T. Perry, G.A. Pierro, G. Polese, T. Ruggles, A. Savin, A. Sharma, N. Smith, W.H. Smith, D. Taylor, N. Woods

†: Deceased

1: Also at Vienna University of Technology, Vienna, Austria

2: Also at State Key Laboratory of Nuclear Physics and Technology, Peking University, Beijing, China

3: Also at Institut Pluridisciplinaire Hubert Curien, Université de Strasbourg, Université de

- Haute Alsace Mulhouse, CNRS/IN2P3, Strasbourg, France
- 4: Also at Universidade Estadual de Campinas, Campinas, Brazil
- 5: Also at Centre National de la Recherche Scientifique (CNRS) - IN2P3, Paris, France
- 6: Also at Université Libre de Bruxelles, Bruxelles, Belgium
- 7: Also at Deutsches Elektronen-Synchrotron, Hamburg, Germany
- 8: Also at Joint Institute for Nuclear Research, Dubna, Russia
- 9: Also at Suez University, Suez, Egypt
- 10: Now at British University in Egypt, Cairo, Egypt
- 11: Also at Ain Shams University, Cairo, Egypt
- 12: Also at Cairo University, Cairo, Egypt
- 13: Now at Helwan University, Cairo, Egypt
- 14: Also at Université de Haute Alsace, Mulhouse, France
- 15: Also at CERN, European Organization for Nuclear Research, Geneva, Switzerland
- 16: Also at Skobeltsyn Institute of Nuclear Physics, Lomonosov Moscow State University, Moscow, Russia
- 17: Also at RWTH Aachen University, III. Physikalisches Institut A, Aachen, Germany
- 18: Also at University of Hamburg, Hamburg, Germany
- 19: Also at Brandenburg University of Technology, Cottbus, Germany
- 20: Also at Institute of Nuclear Research ATOMKI, Debrecen, Hungary
- 21: Also at MTA-ELTE Lendület CMS Particle and Nuclear Physics Group, Eötvös Loránd University, Budapest, Hungary
- 22: Also at University of Debrecen, Debrecen, Hungary
- 23: Also at Indian Institute of Science Education and Research, Bhopal, India
- 24: Also at Institute of Physics, Bhubaneswar, India
- 25: Also at University of Visva-Bharati, Santiniketan, India
- 26: Also at University of Ruhuna, Matara, Sri Lanka
- 27: Also at Isfahan University of Technology, Isfahan, Iran
- 28: Also at University of Tehran, Department of Engineering Science, Tehran, Iran
- 29: Also at Plasma Physics Research Center, Science and Research Branch, Islamic Azad University, Tehran, Iran
- 30: Also at Laboratori Nazionali di Legnaro dell'INFN, Legnaro, Italy
- 31: Also at Università degli Studi di Siena, Siena, Italy
- 32: Also at Purdue University, West Lafayette, USA
- 33: Also at International Islamic University of Malaysia, Kuala Lumpur, Malaysia
- 34: Also at Malaysian Nuclear Agency, MOSTI, Kajang, Malaysia
- 35: Also at Consejo Nacional de Ciencia y Tecnología, Mexico city, Mexico
- 36: Also at Warsaw University of Technology, Institute of Electronic Systems, Warsaw, Poland
- 37: Also at Institute for Nuclear Research, Moscow, Russia
- 38: Now at National Research Nuclear University 'Moscow Engineering Physics Institute' (MEPhI), Moscow, Russia
- 39: Also at St. Petersburg State Polytechnical University, St. Petersburg, Russia
- 40: Also at University of Florida, Gainesville, USA
- 41: Also at P.N. Lebedev Physical Institute, Moscow, Russia
- 42: Also at California Institute of Technology, Pasadena, USA
- 43: Also at Faculty of Physics, University of Belgrade, Belgrade, Serbia
- 44: Also at INFN Sezione di Roma; Università di Roma, Roma, Italy
- 45: Also at National Technical University of Athens, Athens, Greece
- 46: Also at Scuola Normale e Sezione dell'INFN, Pisa, Italy
- 47: Also at National and Kapodistrian University of Athens, Athens, Greece

- 48: Also at Riga Technical University, Riga, Latvia
49: Also at Institute for Theoretical and Experimental Physics, Moscow, Russia
50: Also at Albert Einstein Center for Fundamental Physics, Bern, Switzerland
51: Also at Adiyaman University, Adiyaman, Turkey
52: Also at Mersin University, Mersin, Turkey
53: Also at Cag University, Mersin, Turkey
54: Also at Piri Reis University, Istanbul, Turkey
55: Also at Gaziosmanpasa University, Tokat, Turkey
56: Also at Ozyegin University, Istanbul, Turkey
57: Also at Izmir Institute of Technology, Izmir, Turkey
58: Also at Marmara University, Istanbul, Turkey
59: Also at Kafkas University, Kars, Turkey
60: Also at Istanbul Bilgi University, Istanbul, Turkey
61: Also at Yildiz Technical University, Istanbul, Turkey
62: Also at Hacettepe University, Ankara, Turkey
63: Also at Rutherford Appleton Laboratory, Didcot, United Kingdom
64: Also at School of Physics and Astronomy, University of Southampton, Southampton, United Kingdom
65: Also at Instituto de Astrofísica de Canarias, La Laguna, Spain
66: Also at Utah Valley University, Orem, USA
67: Also at University of Belgrade, Faculty of Physics and Vinca Institute of Nuclear Sciences, Belgrade, Serbia
68: Also at Facoltà Ingegneria, Università di Roma, Roma, Italy
69: Also at Argonne National Laboratory, Argonne, USA
70: Also at Erzincan University, Erzincan, Turkey
71: Also at Mimar Sinan University, Istanbul, Istanbul, Turkey
72: Also at Texas A&M University at Qatar, Doha, Qatar
73: Also at Kyungpook National University, Daegu, Korea